

Double White Dwarf Mergers as Progenitors of Long-Period Transients

Manuel Malheiro^a, Sarah V. Borges^b, Jaziel G. Coelho^{c,d}, Khashayar Kianfar^a, Ronaldo V. Lobato^{e,f}, Edson Otoniel^g, Jorge A. Rueda^{f,h,i,j}, Manoel F. Sousa^k, Fridolin Weber^{l,m}

^aDepartamento de Física, Instituto Tecnológico de Aeronáutica, Praça Marechal Eduardo Gomes 50, São José dos Campos, 12228-900, São Paulo, Brazil

^bDepartment of Physics and Astronomy, University of Wisconsin-Milwaukee, 3135 North Maryland Avenue, Milwaukee, 53211, WI, USA

^cNúcleo de Astrofísica e Cosmologia (Cosmo-Ufes) & Departamento de Física, Universidade Federal do Espírito Santo, Espírito Santo, Brazil

^dDivisão de Astrofísica, Instituto Nacional de Pesquisas Espaciais, Brazil

^eCentro Brasileiro de Pesquisas Físicas, Rua Dr. Xavier Sigaud, 150, Rio de Janeiro, 22290-180, RJ, Brazil

^fICRANet, Piazza della Repubblica 10, Pescara, 65122, Italy

^gUniversidade Federal do Cariri, Instituto de Formação de Educadores, Brazil

^hICRA, Dip. di Fisica, Italy

ⁱICRANet-Ferrara, Ferrara, Italy

^jINAF, Italy

^kInstituto de Física de São Carlos, Universidade de São Paulo, Av. Trabalhador São-carlense 400, São Carlos, Brazil

^lDepartment of Physics, San Diego State University, San Diego, California 92182, USA

^mDepartment of Physics, University of California at San Diego, La Jolla, California 92093, USA

arXiv:2603.08416v1 [astro-ph.HE] 9 Mar 2026

Abstract

There is an ongoing discussion in the literature on the nature of long-period transients (LPTs), radio-emitting sources with periods ranging from hundreds to tens of thousands of seconds. Although some of these objects have been identified as white dwarf (WD) + M-dwarf binaries, this description currently does not fit the entire class. An example is GLEAM-X J162759.5–523504.3 (hereafter GLEAM-X J1627–5235), with a period of 1091 s, for which the lack of an optical counterpart disfavors the presence of such a binary system. In this case, GLEAM-X J1627–5235 could be interpreted as an isolated, massive, fast-rotating, and highly magnetized ($\sim 10^9$ G) WD pulsar. Its properties are consistent with a carbon–oxygen WD of mass $\sim 1.3 M_{\odot}$ and radius ~ 2500 km, possibly supported by small-scale multipolar magnetosphere structures that keep it above the death line for WD-pulsars. We assess a double WD merger origin, modeling the post-merger rotational evolution under accretion, propeller, and magnetic braking torques. We find rotational age of ~ 572 Myr for GLEAM-X J1627–5235, i.e., the post-merger time required to reach its observed period. This result is consistent with current optical upper limits for GLEAM-X J1627–5235 and support the WD pulsar interpretation for this source. We also discuss how the same model can apply to other LPTs.

Keywords: Radio Pulsars, Long-Period Transients, White Dwarfs, GLEAM-X J1627–5235

1. Introduction

Since their discovery (Hewish et al., 1968), neutron star (NS) pulsars have attracted interest due to their extreme physics, including the densest matter known, intense magnetic fields, and rapid rotation. Their spin periods can reach milliseconds ($\Omega = 2\pi/P \sim \text{a few} \times 10^3, \text{ rad, s}^{-1}$), which implies both a deep gravitational potential $\sim (GM\Omega)^{1/3} \sim 0.1c^2$ and a compact radius of order ~ 15 km. Pulsar emission, however, may not be exclusive to NSs: the WD in the binary AR Scorpii (AR Sco), with a rotation period of 1.97 minutes, and pulsed emissions across a wide spectrum of frequencies, has been proposed to be a WD-pulsar (Marsh et al., 2016). The spindown luminosity of AR Sco exceeds by more than one order of magnitude the observed X-ray luminosity, as in traditionally rotation-powered pulsars, and the absence of accretion signatures suggests this classification as a plausible emission mechanism for AR Sco (Buckley et al., 2017). More recently, a counterpart to

AR Sco has emerged, identified within the system J191213.72–441045.1 (hereafter J1912–4410), exhibiting pulsed emission with a period of 5.30 min (Pelisoli et al., 2023).

In this context, long-period radio transients (LPTs) are a new class whose properties place them in an ambiguous position relative to whether they are NSs or WDs (or even something else entirely, e.g., Baumgarte and Shapiro, 2024; Zhou et al., 2025). They have emission periods ranging from 421 s (CHIME J0630+25; Dong et al., 2024) to 6.5 hours (ASKAP J1839-0756; Lee et al., 2025). Their nature has sparked considerable debate, as both NS and WD interpretations face significant challenges (e.g., Rea et al., 2022; Katz, 2022; Loeb and Maoz, 2022; Hurley-Walker et al., 2023a). For NSs, population-synthesis studies disfavor a population of isolated pulsars with spin periods of order 10^3 s (Rea et al., 2024). For WDs, although coherent radio emission has long been predicted in theory, it had not been observationally established prior to the discovery of this class.

The discoveries of GLEAM-X J0704–37 (Hurley-Walker et al., 2024) and ILT J1101+5521 (de Ruiter et al., 2025), both

Email address: svborges@uwm.edu (Sarah V. Borges)

confirmed WD+M-dwarf binaries, strengthened the case for them being WDs. In this case, they are potential WD pulsars and could have a similar emission mechanism to AR Sco and J1912–4410, in which the pulsed emission is likely amplified due to interactions of the WD magnetic field with winds coming from the companion (Geng et al., 2016), and not from curvature or synchrotron emission like for NS pulsars. Thus, binarity may be an essential feature in the observation of WD pulsars and may explain why LPTs with confirmed nature have been detected in WDs from binaries. Unfortunately, this binary WD pulsar model cannot explain the entire class. In particular, GLEAM-X J162759.5–523504.3 (hereafter, GLEAM-X J1627–5235) has optical MUSE/VLT observations that disfavor the presence of an emission exactly similar to LPTs known to be WDs (Lyman et al., 2025). More specifically, the optical limits place strong constraints on the presence of a WD+M-dwarf binary at the given distance, which could be reconciled if the distance to the source has been underestimated, but increasing the distance would further increase the radio luminosity, which is already significantly brighter than for WD+M-dwarf LPTs.

GLEAM-X J1627–5235 has a rotation period of 1091 s and a spindown rate upper limit $\dot{P} \leq 1.2 \times 10^{-9} \text{ s s}^{-1}$ (Hurley-Walker et al., 2022a). Moreover, unlike confirmed binary LPTs, in which the few-hour period is likely orbital, the period of GLEAM-X J1627–5235 is too short for a WD+M-dwarf binary and is possibly the object spin period. Observationally, its radio emission shares characteristics with that of GLEAM-X J0704–37, including high linear polarization, short-duty-cycle bursts, and millisecond-scale microstructure. A NS interpretation for these long-period objects, however, would require nonphysical magnetic fields ($\gtrsim 10^{17} \text{ G}$, Hurley-Walker et al., 2024). If interpreted as an isolated WD, it can be a fast-rotating, highly magnetized remnant with a mass of $\sim 1.3 M_{\odot}$, period $\sim 10^3 \text{ s}$, and magnetic fields $\sim 10^9 \text{ G}$, consistent with double WD merger products. More importantly, due to its extreme parameters, this post-merger massive isolated WD can be above the death line for a WD-pulsar and does not need to rely on the interactions with the companion to have a pulsar emission.

Although the WD interpretation remains indirect due to the absence of optical counterparts or measured spindown rates, our modeling yields falsifiable predictions. If confirmed, the merger origin would support the hypothesis that strong magnetization is a natural outcome of the merger dynamics (García-Berro et al., 2012). These findings reinforce the scenario explored here, in which some LPTs may originate from double WD mergers, producing isolated, fast-rotating, highly magnetized WDs capable of coherent radio emission over gigayear timescales.

The paper is structured as follows. In Section 2, we discuss the current population of observed WDs with similar parameters and the ongoing debate regarding their possible origin in double WD mergers. Because LPTs are radio emitters, much of the recent literature has focused on the so-called pulsar death lines and limits to the spindown luminosity (e.g., Rea et al., 2022; Tong, 2023a,b). We revisit these radio emission constraints in Section 3 to assess the physical conditions required for coherent radio activity in WD pulsars. In this discussion of

the death-line, we include all LPTs in which this model can be applied. In Section 4, we examine the post-merger cooling evolution of GLEAM-X J1627–5235 and compare with the current upper limits from VLT/MUSE. Section 5 presents our rotational evolution models based on a double WD merger scenario, incorporating accretion, propeller, and magnetic braking torques. As an example, we applied this model to two LPTs, GLEAM-X J1627–5235 and GPM J1839-10. In Section 6, we provide the maximum expected optical magnitudes for LPTs as isolated WDs, to guide future observations. Finally, in Section 7, we discuss and summarize our results.

2. Observation of massive, fast-rotating, highly magnetic WDs and their post-merger origins

WDs can exhibit magnetic fields with intensities ranging from 10^3 G to 10^9 G (see, e.g., Külebi et al., 2009; Kuelebi et al., 2010; Kepler et al., 2013; Kepler et al., 2015; Amorim et al., 2023; Ferrario et al., 2015, for a review). They can also show rotational periods spanning from seconds to hours. Among the fastest rotation periods ever observed is that of LAMOST J0240.51+1952, with an extraordinary rotation period of 24.93 s (Pelisoli et al., 2022), and CTCV J2056-3014, with a period of 29.6 s (Lopes de Oliveira et al., 2020; Otoniel et al., 2021). The presence of a strong magnetic field and rapid rotation provides strong evidence for past and current binary interactions. In such systems, the progenitors likely passed through a common-envelope evolution (CEE) phase, which is responsible for forming close binaries (see, e.g. Iaconi and De Marco, 2019; Ivanova et al., 2020; Borges, 2026). Subsequent episodes of mass transfer can both spin up the WD by transferring angular momentum and amplify magnetic fields via crystallization and rotation-driven dynamo processes (Schreiber et al., 2021).

There is also a population of magnetic, isolated, and massive WDs that has been identified across several investigations (Althaus et al., 2005, 2007; Hermes et al., 2013; Kepler et al., 2016; Curd et al., 2017; Gentile Fusillo et al., 2018; Jiménez-Esteban et al., 2018; Camisassa et al., 2019). Notable examples include ZTF J1901+1458, with $M \approx 1.31 M_{\odot}$ and $B \approx (6.0\text{--}9.0) \times 10^8 \text{ G}$ (Caiazzo et al., 2021), and PG 1031+234, which holds the record for the highest magnetic field detected, $B \approx 10^9 \text{ G}$ (Schmidt et al., 1986; Külebi et al., 2009). In this case, double WD mergers, a more extreme form of binary interaction, have long been proposed as a natural explanation for the origin of these objects (Wickramasinghe and Ferrario, 2000). Previous studies have shown that magnetic WDs are, on average, more massive than their non-magnetic counterparts, which agrees with this merger origin interpretation (Kepler et al., 2013)

Theoretical work led by numerical simulations shows that mergers can form sub-Chandrasekhar WD central remnants (Benz et al., 1990; Guerrero et al., 2004; Lorén-Aguilar et al., 2009; Longland et al., 2012; Raskin et al., 2012; Zhu et al., 2013; Dan et al., 2014; Becerra et al., 2018). A dynamo process and the high spin due to the total orbital momentum of the merger are expected to be responsible for magnetizing the WD (García-Berro et al., 2012). These mergers are

Table 1: Parameters of LPTs presented in Fig. 1 and some isolated WDs. Columns indicate rotation period (P), spindown rate (\dot{P}), magnetic field (B), mass (M), radius (R), temperature (T), age (τ), distance (d), and extinction in the G-band (A_G). We have not included the distance and extinction for isolated WDs, because they are not relevant to this work.

Sources	P (s)	\dot{P} (10^{-11} s.s $^{-1}$)	B (10^8 G)	M (M_\odot)	R (km)	τ (Myr)	d (kpc)	A_G	Ref.
LPTs									
GLEAM-X J1627	1091.17	< 120	$\leq 6031^a$	1.33 ^c	2500 ^c	$\geq 0.014^d$	1.3 ± 0.5	~ 0.7	(1)
GPM J1839-10	1318.20	< 0.036	$\leq 115^a$	1.33 ^c	2500 ^c	$\geq 58.0^d$	5.7 ± 2.9	~ 3.4	(2)
ASKAP J1935+2148	2225.31	< 12	$\leq 2723^a$	1.33 ^c	2500 ^c	$\geq 0.29^d$	~ 4.85	~ 1.8	(3)
CHIME J0630+25	421.35	0.08	97^a	1.33 ^c	2500 ^c	8.3^d	$0.17^{+0.31}_{-0.10}$	~ 0.3	(4)
DART J1832-0911	2656.24	< 0.9	$\leq 815^a$	1.33 ^c	2500 ^c	$\geq 4.7^d$	4.5 ± 1.2	~ 5.8	(5)
ASKAP J1755-2527	4186.32	< 1	$\leq 1078^a$	1.33 ^c	2500 ^c	$\geq 6.6^d$	~ 4.7	~ 8.9	(6)
Isolated WDs									
J2211+1136	70.32	–	0.15^b	1.27	3210	2600-2900 ^e			(7)
J1252-0234	317.28	–	0.05^b	0.65	8374	1136 ± 95^e			(8)
J1901+1458	416.24	< 1	$6\text{--}9^b$	1.33-1.36	2140	10-100 ^e			(9)
J0317-0853	725.74	–	$1.7\text{--}6.6^b$	1.34	2456	281^{+36}_{-31} e			(10)
J0006+3104	1385	–	$\sim 2.5^b$	1.06	4528	200 ± 10^e			(11)

^a Magnetic field from dipole braking: $B \sin \theta = \sqrt{\frac{3c^3 I \dot{P}}{8\pi^2 R^6}}$, with $M = 1.33 M_\odot$, $R = 2500$ km, $I = \frac{2}{5} MR^2 = 6.61 \times 10^{49}$ g cm 2 , and θ is the angle between the axis of rotation and the magnetic axis. ^b Magnetic field inferred from atmosphere/spectral modeling. ^c: fixed parameter from our model. ^d characteristic age ($\tau_{\text{char}} = P/2\dot{P}$), ^e: cooling age from surface temperature. (1) Hurley-Walker et al. (2022a), (2) Hurley-Walker et al. (2023b), (3) Caleb et al. (2024), (4) Dong et al. (2025a), (5) Wang et al. (2025), (6) Dobie et al. (2024), (7) Kilic et al. (2021b,a), (8) Reding et al. (2020); Gänsicke et al. (2020), (9) Caiazzo et al. (2021), (10) Ferrario et al. (1997); Vennes et al. (2003); Külebi et al. (2010), (11) Guo et al. (2026).

expected to be numerous, with a local universe rate of $(3.7\text{--}6.7) \times 10^5$ Gpc $^{-3}$ yr $^{-1}$ (Maoz and Hallakoun, 2017; Maoz et al., 2018; Sousa et al., 2022), which is 5–8 times larger than that of SN Ia (Ruiter et al., 2009). Therefore, we expect many mergers do not produce SNe Ia (Cheng et al., 2020), some of them lead to metastable super-Chandrasekhar WDs that can form neutron stars by delayed gravitational collapse (Becerra et al., 2018), and finally, some lead to massive, highly magnetized, fast-rotating WDs.

The observed transverse velocities of massive WDs also hint that a non-negligible fraction might have originated from double WD mergers (Cheng et al., 2020). A recent study (Kilic et al., 2023) looked for possible merger remnants among the most massive 25 WDs in a sample of 100 pc from the *Montreal WD Database*, analyzing features such as rapid rotation, high tangential velocities, magnetic properties, and unusual atmospheric compositions, concluding that 14 sources strongly suggest WD mergers or similar phenomena. Toonen et al. (2017) elucidated an additional aspect that bolsters the merger hypothesis. Using WDs within a 20 pc sample and recent data from the *Gaia* space observatory, they showed that the prevalence of WD binaries ($\sim 25\%$) is lower when compared to the occurrence of double systems containing solar-type main-sequence stars ($\sim 50\%$). This discrepancy is consistent with the idea that 10% to 30% of all isolated WDs result from coalescence processes (Toonen et al., 2017).

In terms of rotation, isolated magnetic WDs can occupy two extremes, with spins that are either significantly faster or slower than those of their non-magnetic counterparts. At one end, a number of magnetic WDs exhibit extremely long periods ($>$

100 years), far exceeding the average period of non-magnetic WDs (around a day, Ferrario et al., 2015). On the other hand, recent observations have revealed isolated WDs with very short rotation periods, ranging from seconds to minutes. In particular, SDSS J221+1136 has a spin period of $P = 70.32$ s (Kilic et al., 2021b), and ZTF J1901+1458 has $P = 416.20$ s (Caiazzo et al., 2021). This diversity can be explained by the formation and evolution of post-merger WDs. These objects are initially born as rapid rotators; however, magnetic braking and interactions with the massive disk formed shortly after the merger can efficiently remove angular momentum, in some cases producing periods longer than those of typical isolated non-magnetic WDs. Ultimately, the rotation period of an isolated magnetic WD can span a wide range, depending on its initial period, age, magnetic field strength, and disk properties. Consistent with this picture, recent simulations of the rotational and thermal post-merger evolution of WDs have shown that observed isolated systems, in particular SDSS J221+1136 and ZTF J1901+1458, can be reproduced as products of WD mergers (Sousa et al., 2022).

Table 1 showcases a subset of isolated, fast, and magnetic WDs known in the literature. The rotation period, magnetic field, temperature, and mass have been derived from photometric and spectral analyses, as well as model-atmosphere features. Cooling ages are estimated using evolutionary and cooling models (see Kilic et al., 2021a; Caiazzo et al., 2021; Gänsicke et al., 2020; Külebi et al., 2010, and references therein). In the case of ZTF J1901+1458, the WD radius is derived from photometric and distance measurements, and the mass is obtained from the mass-radius relation. For TMTS J0006+3104,

the radius is determined from spectral energy distribution fitting. For the other WDs, the radius is estimated from the surface gravity, g , i.e., $R = \sqrt{GM/g}$. The spindown rate for these sources remains unknown, except for ZTF J1901+1458, which has an upper limit value for this parameter (see Caiazzo et al., 2021).

Table 1 also presents the observed spin, (upper limit) spindown, distance, and extinction in the G-band for GLEAM-X J1627–5235 and other LPTs that are potential isolated WDs. For the extinction, we considered the objects dispersion measures and the method to obtain A_G ($DM \rightarrow N_H \rightarrow A_V \rightarrow A_G$) described in Sec. 4. We include all LPTs that have measured spindown limits, no confirmed companion, and periods in the order of $\sim 10^3$ s, which was chosen to guarantee that the minimum magnetic field for the object to be above the death-line of WD pulsars is around 10^9 G. We also included the (upper limit) magnetic field, determined from the dipole braking formulae; the (lower limit of) the characteristic age; and the mass and radius, which are fixed parameters in our model. We have not included the LPTs ILT J1101+5521, GLEAM-X J0704-36 and ASKAP J1448-6856 due to their WD+M-dwarf binary nature (Rodríguez, 2025; de Ruiter et al., 2025; Anumarlapudi et al., 2025), GCRT J1745-3009 due to the lack of spin down upper limits (Hyman et al., 2005), ILT J1634+44 because this object is spinning-up (Dong et al., 2025b), and ASKAP J1839-0756 due to its high period (Lee et al., 2025).

When we began this work, we included GPM J1839–10 as a candidate isolated WD. However, it has recently been proposed to reside in a binary system, despite the lack of a confirmed optical counterpart, based on the detection of a secondary period of 8.75 h in radio in addition to the primary period of 1318 s (Horváth et al., 2025). In this interpretation, the longer period corresponds to the orbital period, while the shorter period is a beat period between the orbital period and the WD spin period (1265 s). We opt to keep this object in our sample with appropriate caveats. We first note that GPM J1839–10 may be a fast, massive, and magnetic WD in a binary system. REJ 0317–853, for example, is in a wide binary system, yet it is a strong candidate to be formed through a WD+WD merger due to its extreme parameters (see Table 1. Also Külebi et al., 2010).

In close binaries, a post-merger WD can be present in several ways. One possibility is a CEE occurring in the still-triple system, in which two WDs are in a close binary orbiting a giant. In this case, the two WDs can merge during the event (see, e.g., Glanz and Perets, 2021). The final product would be a close binary with a massive WD and the core of the giant (either another WD or a hot subdwarf). In general, the biggest indication of a merger is the potential high mass for the WD ($\gtrsim 1.3 M_\odot$), given that high magnetic fields and fast periods can also be explained by other, less extreme binary interactions. Thus, until the origin of the secondary period is confirmed to be orbital and the nature and masses of the objects are determined, the merger nature of GPM J1839–10 remains possible, so we retain this object in our analysis.

3. Death lines for WD-pulsar

We now recall the traditional death lines for pulsar radio emission and apply them to WDs. The radio emission models consider the acceleration of electrons and positrons (e^\pm) to extreme energies, such that the radiation originated by these particles could create new e^\pm , which in a sequence creates new ones, leading to a cascade. This avalanche is expected to produce coherent radio-wave flux. We refer the reader to Philippov and Kramer (2022) for a recent review. Therefore, traditionally, the minimum condition for pulsar radio emission is that the pulsar magnetosphere produces the first generation of pairs.

The basics of such a process roots in the *polar-cap* model by Goldreich and Julian (1969); Sturrock (1971); Ruderman and Sutherland (1975). The electric field component along the *open* magnetic field lines does not vanish in the pulsar *gap*, accelerating charged particles to sufficiently high Lorentz factor to produce γ -rays by synchro-curvature radiation. Photons interact with the magnetic field, leading to the first generation of pairs, i.e., $\gamma + B \rightarrow e^+ e^-$ (Sturrock, 1971; Ruderman and Sutherland, 1975). The electric potential drop along an open field line above the surface is $\Delta V = B_s \Omega h^2 / c$ where $h \ll R$, being h the gap thickness and R the stellar radius (see Eqs. A7 in Ruderman and Sutherland, 1975)). The condition for pair production by photon-magnetic field interaction is (Sturrock, 1971; Chen and Ruderman, 1993)

$$\frac{3}{2} \gamma^3 \frac{\hbar}{2mcr_c} \frac{h}{r_c} \frac{B_s}{B_g} \approx \frac{1}{15}, \quad (1)$$

where r_c is the curvature radius of the magnetic field lines, $B_g = m^2 c^3 / (e\hbar) = 4.42 \times 10^{13}$ G, B_s the magnetic field on the surface, $\gamma = e\Delta V / (mc^2)$ the electron's Lorentz factor, and m its rest-mass. With all the above, one can express the gap thickness and the electric potential drop in the gap as a function of the other pulsar parameters, i.e.,

$$h = 4.76 \times 10^6 \left(\frac{r_c}{10^6 \text{ cm}} \right)^{2/7} \left(\frac{P}{10^3 \text{ s}} \right)^{3/7} \times \left(\frac{B_s}{10^9 \text{ G}} \right)^{-4/7} \text{ cm}, \quad (2)$$

$$e\Delta V = 1.42 \times 10^{12} \left(\frac{r_c}{10^6 \text{ cm}} \right)^{4/7} \left(\frac{P}{10^3 \text{ s}} \right)^{-1/7} \times \left(\frac{B_s}{10^9 \text{ G}} \right)^{-1/7} \text{ eV}. \quad (3)$$

The potential drop reaches its maximum value $\Delta V_{\max} = B_s R^3 \Omega^2 / c^2$ for the gap thickness of a magnetic dipole, which is given by the polar cap size, $r_p \approx R \theta_p$, being $\theta_p = \arcsin(\sqrt{R/r_{lc}}) \approx \sqrt{R/r_{lc}}$ the polar cap angular size, i.e., the angular size from the rotation axis to the last open field line, with $r_{lc} = c/\Omega$ the light cylinder radius. Therefore, $h_{\max} = r_p = R \sqrt{R/r_{lc}}$. The condition that $h < h_{\max}$, or equivalently $\Delta V < \Delta V_{\max}$, sets the WD-pulsar's death line, so a lower limit to the very curved magnetic field for pair creation by photon-

magnetic field interaction, i.e.,

$$B_s \geq 6.02 \times 10^{10} \left(\frac{10^8 \text{ cm}}{R} \right)^{21/8} \left(\frac{r_c}{10^6 \text{ cm}} \right)^{1/2} \times \left(\frac{P}{10^3 \text{ s}} \right)^{13/8} \text{ G.} \quad (4)$$

Figure 1.a shows the WD pulsar death lines set by Eq. (4) for $R = 2500 \text{ km}$ ($M \approx 1.3M_\odot$), $h = h_{\text{max}} = r_p$, and two values of the curvature radius, $r_c = 0.001R$ and $r_c = 0.01R$. Here R is the WD stellar radius. Radii of curvature $r_c \ll R$ do not describe a global centered-dipole/open-line geometry, but rather local, small-scale, near-surface multipolar spot-like magnetic structures anchored in the outer layers of the WD. In such non-dipolar polar-cap regions, neighboring opposite-polarity flux bundles and strong higher-order multipoles components (or an offset dipole) can bend open lines on scales much smaller than R , even $r_c \sim 10^{-3}\text{--}10^{-2}R$, also enhancing pair creation (see, e.g., Gil and Mitra, 2001; Harding and Muslimov, 2011, for discussions of this effect in pulsars). The source points are for the LPTs parameters (rotation period and magnetic field) in Table 1. Figure 1.b shows the physical situation from the potential drop viewpoint, i.e., it plots the maximum potential drop $e\Delta V_{\text{max}}$ using the death line shown in Fig. 1.a, and using the observed magnetic field value reported in Table 1. The condition for radio emission imposes that the corresponding source lies above the gray-filled region.

Figure 1 suggests constraints on the WD magnetosphere parameters for the radio emission of LPTs. The figure indicates the upper limits to the magnetic field of these sources given by the magnetic dipole braking model in Table 1. It arises that, as expected, the magnetic fields must be a few 10^9 G for WDs with periods around 10^3 s . For the only LPT with measured spindown rate (not an upper limit), CHIME J0630+25 has an estimated magnetic field of $9.7 \times 10^9 \text{ G}$ from dipole braking of a WD and is expected to lie above the death line. Moreover, the magnetospheric structure may be complex, exhibiting small-scale multipolar structure. As clarified above (see discussion around Fig. 1), the small r_c values are interpreted as local curvature in a multipolar surface field, not as the curvature of a global dipole. In other words, the WDs would require a complex, intense multipolar field with a small r_c . For higher-order multipoles, such as quadrupolar and octupolar fields, the strength of B_s becomes significantly higher than the inferred dipole field, and the geometry of the field becomes much more convoluted. The curvature radius can be even smaller than the stellar radius in a highly localized spot. Previous work has shown that very small radii of curvature, i.e., small-scale sunspot-like fields, can shift the curvature radiation death line to much lower surface magnetic field values (Gil and Mitra, 2001). A modest offset of the dipole, which creates an asymmetric polar cap, can also dramatically enhance pair production (Harding and Muslimov, 2011). Also, LPTs like GLEAM-X J1627–5235 likely represent a specific ultra-massive subset of WD population, because the death line magnetic field requirement scales with $R^{-21/8}$. Using the radius of a massive WD (2500 km) instead of a standard one (6000 km) reduces the re-

quired magnetic field strength by nearly one order of magnitude for the same period. In short, realistic field geometry and acceleration physics can markedly relax the death-line cutoff. We should consider the above as estimates since more reliable values of the death line for WD-pulsars require the nontrivial analysis of the possible effects by the magnetic axis inclination relative to the rotation axis, magnetic axis shift from the center, the polar cap size, magnetic field geometry, the charged particle density flow, general relativity, and additional complications (see, e.g., Harding and Muslimov, 2011; Cerutti et al., 2016; Bilous et al., 2019; Pétri, 2019; de Lima et al., 2020, 2024; Coelho et al., 2021; Beskin and Litvinov, 2022; Beskin and Istomin, 2022, , and references therein), the death-line is not a universal boundary, but is highly sensitive to the stellar radius and curvature of the magnetic field. Independently, it is worth emphasizing that these simple estimates yield reasonable estimates for massive, fast-rotating, highly magnetized WDs, including a light cylinder radius comparable to the star’s size. On the other hand, applying the same model to a neutron star leads to ultrastrong magnetic fields of $10^{16}\text{--}10^{17} \text{ G}$ and a light cylinder radius a million times the star radius, which seem not to fit within a reasonable picture (see, e.g., discussion in Kaspi, 2023). Furthermore, Rea et al. (2024) notes that for NSs, population synthesis cannot explain the number of ultra-long period sources without unrealistic rates of zero magnetic field decay.

Massive WDs ($>1.3 M_\odot$) are unlikely to form from single-star evolution due to the mass-loss constraints and are almost certainly the products of double white dwarfs mergers or significant binary interaction. Simulations of binary WD mergers show that the process creates a central core surrounded by a hot, differentially rotating envelope and a massive debris disk. Differential rotation is the primary engine for dynamo application. Magnetic fields generated by dynamos in a turbulent post-merger environment are inherently complex and fragmented, and such dynamos naturally distribute magnetic power across many multipolar modes rather than focusing it solely in dipole mode (Castro-Tapia et al., 2026). In the post-merger cooling phase, magnetic fields can undergo Hall drift or re-merger from the crust, potentially creating small-scale, intense ‘spots’ of magnetic field at the polar caps. These spots are physical manifestations of the multipolar components required to lower the curvature radius. The evidence of the complexity of B is not limited to theory. Multi-wavelength studies of millisecond pulsars and magnetars have frequently found that a pure dipole field fails to explain pulse profiles and X-ray hotspots, requiring multipolar surface components to fit data (Lockhart et al., 2019). The transient nature of GLEAM-X J1627–5235 (active for months) versus GPM J1839–10 (active for decades) suggests a highly variable magnetospheric state. The small-scale multipolar structures that enable pair production may be subject to Hall-driven evolution or reconnection, which can periodically quench or ignite the radio emission. Due to this cycle, population synthesis, such as demonstrated in Rea et al. (2024), would find it difficult to explain emission, since it models a steady-state dipole rather than a dynamic, multipole-dominated system.

Our model predicts rotational ages of 390 Myr and 572 Myr

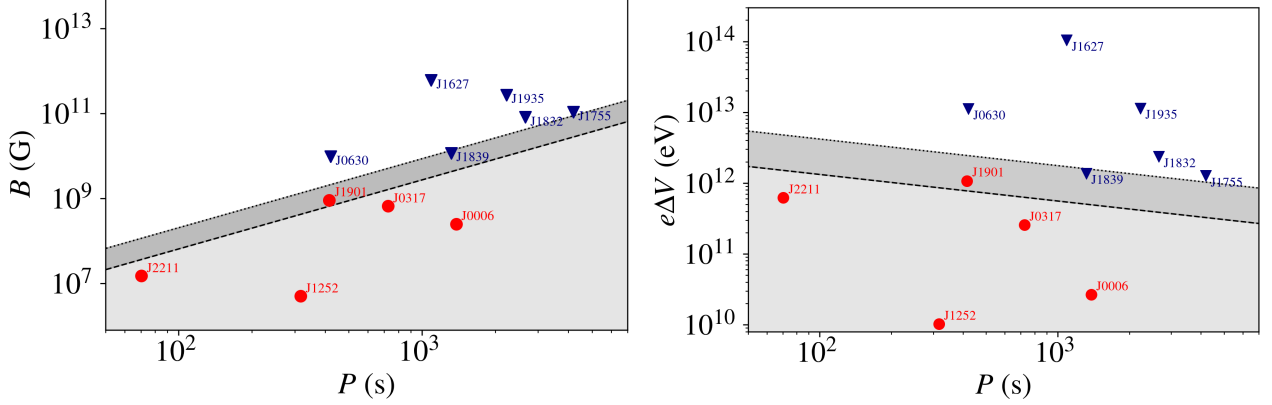


Figure 1: **Left:** Magnetic field limits set by the death line for WD-pulsars. Black-dashed curve: $r_c/R = 0.001$. Black-dotted curve: $r_c/R = 0.01$. Other parameters are $R = 2500$ km ($M \approx 1.3 M_\odot$) and $h = h_{\max} = r_p$. Period and magnetic field values of magnetic WDs (red circles) are from Table 1, while the upper limits of magnetic field for LPTs (blue triangles) are from Table 1. Exceptionally, CHIME J0630+25 has a measured spindown rate, and thus the magnetic field is not an upper limit but an estimate based on dipole braking. **Right:** Electric potential drop limits set by the death line for WD-pulsars. Black-dashed curve: $r_c/R = 0.001$. Black-dotted curve: $r_c/R = 0.01$. Other parameters are as in the left panel.

for GPM J1839–10 and GLEAM-X J1627–5235, and the consistency with cooling age constraint for $1.33 M_\odot$ WD larger than 556 Myr supports multi-wavelength constraints, as follows in the next sections. It demonstrates that the post-merger WD, once it has slowed to the observed rotational period, could have cooled sufficiently to be undetectable in optical observations, indicating that the specific sub-population of the merger satisfies all current multi-wavelength constraints.

4. Minimum Age of GLEAM-X J1627–5235 from Optical Upper Limits

Optical observations provide crucial insights into the origin and nature of compact objects. For instance, optical spectroscopy can confirm a merger origin, as demonstrated by WD J0551+4135, which exhibits carbon and hydrogen absorption lines (Hollands et al., 2020). Zeeman splitting of these lines allows estimation of the surface magnetic field, while polarimetry observations constrain the dipole field strength and geometry (e.g., Buckley et al., 2017; du Plessis et al., 2022). Unfortunately, such data are unavailable for the two sources analyzed here. However, upper limits on GLEAM-X J1627–5235 can be used to constrain the object’s age under a WD model.

Lyman et al. (2025) report a 5σ upper limit of 24.4 mag from VLT/MUSE observations for GLEAM-X J1627–5235. Although upper limits in other bands exist (see Rea et al., 2022), the VLT/MUSE data provide the strongest constraint, so we focus on them for the age estimate. As noted by Lyman et al. (2025), the MUSE wavelength range broadly overlaps with the *Gaia* *G* band, except for a small gap between 4000–4700 Å. We therefore adopt this upper limit as the *G*-band magnitude (m_G), allowing straightforward use of *Gaia* passbands in WD cooling models. To derive the minimum age, we employ cooling models for massive WDs: for $M > 1.30 M_\odot$, we use relativistic carbon-oxygen curves from Althaus et al. (2023), while for $1.10 < M < 1.30 M_\odot$, we adopt the H-rich, $Z = 0.001$ curve

from Camisassa et al. (2022), chosen to minimize discontinuities at $1.30 M_\odot$.

We estimate the V-band extinction (A_V) using two complementary approaches: (1) via empirical relations between dispersion measure (DM), photoelectric absorption column density (N_H), and A_V ; and (2) by extracting A_V directly from a 3D extinction map (e.g. Zhang et al., 2023) using the assumed distance (estimated from DM). Both methods rely on the connection between distance, DM, N_H , and A_V . By tracing two distinct pathways, $\text{DM} \rightarrow \text{distance} \rightarrow A_V$, and $\text{DM} \rightarrow N_H \rightarrow A_V$, we can cross-check our extinction estimates.

For the first approach, we use the relation between DM and N_H (He et al., 2013):

$$N_H = (0.30^{+0.13}_{-0.09}, \text{DM}) \times 10^{20} \text{ cm}^{-2}, \quad (5)$$

and the correlation between N_H and A_V (Zhu et al., 2017):

$$A_V = (4.81 \pm 0.05) \times 10^{-22} N_H. \quad (6)$$

For GLEAM-X J1627–5235, with $\text{DM} = 57 \pm 1 \text{ pc cm}^{-3}$ (Hurley-Walker et al., 2022b), we find $A_V = 0.82^{+0.04}_{-0.03}$. Using the second method, assuming a distance of $1.3 \pm 0.5 \text{ kpc}$ (Hurley-Walker et al., 2022b) and the extinction map of Xiangyu and Green (2024), we find $A_V \sim 0.9$. Unless the source lies behind a local dust cloud, the agreement between the two methods indicates that the DM-based estimate provides a reasonably constrained value. For simplicity, we adopt the first method ($\text{DM} \rightarrow N_H \rightarrow A_V$) for subsequent calculations, as it simplifies uncertainty propagation by making A_V independent of distance.

Finally, we estimate A_G , the extinction in the *G* band, as $A_G = 0.87 A_V$ (Cardelli et al., 1989). The apparent *G*-band magnitude m_G is then:

$$m_G = M_G + 5 \log_{10}(d_{\text{pc}}) - 5 + A_G. \quad (7)$$

By comparing M_G from the cooling models with the observed limit $m_G = 24.4 \text{ mag}$, we estimate the cooling age

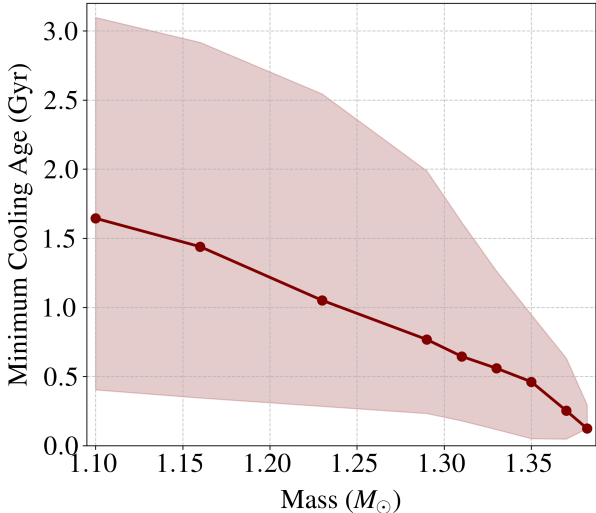


Figure 2: Curve of the minimum age from the optical upper limits for each mass between 1.10 and 1.382 M_{\odot} (blue) for GLEAM-X J1627–5235. The shaded area reflects uncertainties arising from distance and extinction.

for masses between 1.10 and 1.382 M_{\odot} . Figure 2 shows that the minimum age for GLEAM-X J1627–5235 ranges from 100 Myr (1.382 M_{\odot}) to 1.6 Gyr (1.10 M_{\odot}), not including uncertainties, which are shown in the figure only. This age is consistent with recently discovered fast massive WDs like J2211+1136 (2.61–2.85 Gyr) and J1901+1458 (10–100 Myr, Sousa et al., 2022).

5. Post-merger rotational evolution

The merger of two WDs can lead to various outcomes, mainly determined by the masses and compositions of the binary components. These include SN Ia, NSs formed by collapse, and several classes of hydrogen-deficient stars. A schematic overview of the possible outcomes as a function of WD masses is presented in Dan et al. (2014). Among these channels, mergers of two CO WDs are expected to be the most likely pathway to form stable, massive, rapidly rotating, and strongly magnetic WDs in the merger aftermath. Mergers involving oxygen-neon WDs are unlikely to produce a stable massive WD, as their pre-merger masses already exceed $\sim 1 M_{\odot}$ and only a small amount of mass is expected to be ejected during the event (Lorén-Aguilar et al., 2009). Therefore, this scenario most likely forms an NS, given that a long-lasting stable WD remnant would require a low-mass secondary. Mergers between a CO WD and a helium (He) WD may instead produce extreme helium stars or R Coronae Borealis stars (Zhang et al., 2014), while double He WD mergers are thought to form hot subdwarfs (Heber, 2009).

However, not always will CO+CO WD mergers form stable massive WDs, since the outcome depends on the masses of the original WDs. Mergers in which the total mass exceeds the Chandrasekhar limit are generally expected to evolve toward either an SN Ia (Becerra et al., 2018; Neopane et al.,

2022) or NS (Schwab et al., 2016; Becerra et al., 2018). Previous works show that for systems with sub-Chandrasekhar total mass, the merger of a mass-symmetric binary can end as an SN Ia (van Kerkwijk et al., 2010), while, in the case of mass-asymmetry, the secondary is tidally disrupted. In the latter case, the final outcome will be a central WD remnant with a mass approximately equal to the mass of the primary that remains undisturbed, surrounded by a hot envelope made up of approximately half of the secondary. This envelope is surrounded by a rapidly rotating Keplerian disk that contains most of the remaining mass of the less massive WD (see, e.g., Lorén-Aguilar et al., 2009). The envelope is rapidly accreted onto the central WD, resulting in a uniformly rotating WD surrounded by a Keplerian disk. In this work, we explore the evolution of this latter system.

We now investigate GPM J1839–10 and GLEAM-X J1627–5235 as merger products. Those two LPTs were chosen as examples, but this model can be applied to other LPTs from Table 1. For this task, we calculate their post-merger rotational evolution using the recent model presented by Sousa et al. (2022). We examine the evolution of rotational dynamics of the central remnant WD assuming accretion and propeller torque, T_{acc} , and magnetic torque, T_{mag} (Menou et al., 1999; Pétri, 2015):

$$T_{\text{acc}} = \dot{M} \sqrt{GMR_m} (1 - \omega), \quad T_{\text{mag}} = -\frac{2}{3} \frac{B^2 R^6 \Omega^3}{c^3} \sin^2 \theta, \quad (8)$$

where θ is the inclination angle of the magnetic dipole moment ($\mu = BR^3$) relative to the WD rotation axis, R_m is the magnetosphere radius given by the Alfvén radius (see, e.g., Pringle and Rees, 1972)

$$R_m = \left(\frac{\mu^2}{\dot{M} \sqrt{2GM}} \right)^{2/7}, \quad (9)$$

and $\omega = \Omega/\Omega_K$ is the *fastness* parameter being $\Omega_K = \sqrt{(GM)/(R_m^3)}$ the Keplerian angular velocity at the radius R_m . When $\omega < 1$, the material accretes on the stellar surface and transfers angular momentum to it. When $\omega > 1$, the system enters the so-called propeller regime, in which the WD loses angular momentum because its centrifugal barrier ejects the infalling mass from the disk. We consider a constant value of M given by the observed WD mass, and assume it to be the mass of the central, uniformly rotating WD remnant. As mentioned above, to this mass contribute the mass of the primary, of the hot envelope, and a fraction of fallback material. As we shall see, the accreted mass from the disk during the post-merger evolution, M_{acc} , is relatively small compared to the total WD mass, so it can be neglected for our purpose. We also assume a constant mass accretion rate, \dot{M} , onto the central WD. These simplifications do not significantly affect our results, since both mass accretion and mass ejection deplete the disk on timescales much shorter than the WD lifetime.

The WD rotation evolves differently depending on the model parameters and initial conditions. Generally, it evolves through three stages before reaching its current rotation period, depending on the fastness parameter value: $\omega > 1$, $\omega \approx 1$, or $\omega < 1$.

Table 2: Values of the initial and derived parameters used in the WD spin-evolution model: mass (M), radius (R), magnetic field (B), accretion rate (\dot{M}), disk mass (M_d), equilibrium period (P_{eq}), time elapsed in *phase I* (Δt_I), *phase II* (Δt_{II}) and *phase III* (Δt_{III}), total rotational evolution time (Δt_{evo}) and spindown rate at the end of evolution (\dot{P}_{evo})

Parameter	GPM J1839-10	GLEAM-X J1627-5235
Initial Parameters		
$M (M_{\odot})$	1.33	1.33
R (km)	2500	2500
B (10^8 G)	10.0	10.0
\dot{M} ($10^{-7} M_{\odot} \text{ yr}^{-1}$)	2.00	3.35
$M_d (M_{\odot})$	0.30	0.30
Derived Parameters		
P_{eq} (s)	1284.8	1030.0
Δt_I (kyr)	4.50	3.51
Δt_{II} (Myr)	1.495	0.892
Δt_{III} (Gyr)	0.388	0.571
Δt_{evo} (Gyr)	0.390	0.572
\dot{P}_{evo} ($10^{-15} \sin^2 \theta \text{ s s}^{-1}$)	2.73	3.30

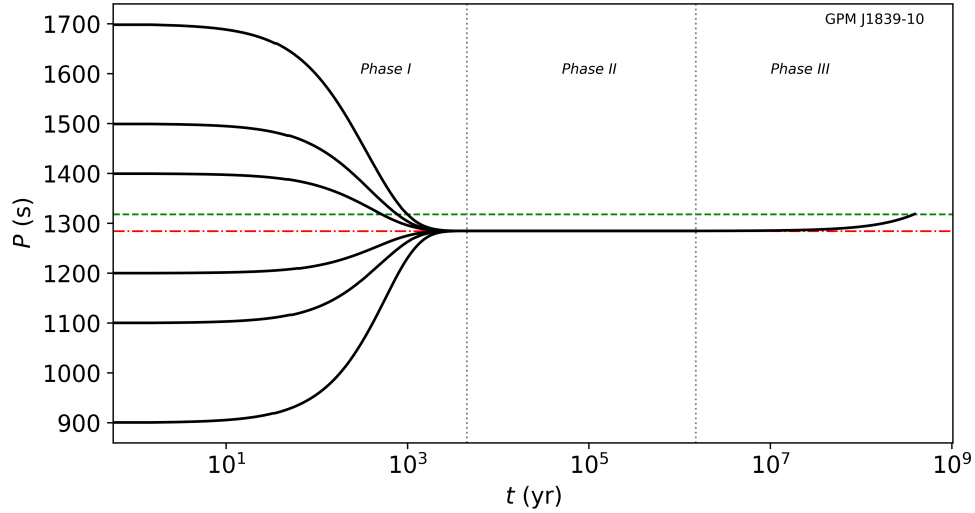


Figure 3: Evolution of the rotation period of GPM J1839-10 for an accretion rate of $\dot{M} = 2.0 \times 10^{-7} M_{\odot} \text{ yr}^{-1}$ and for different values of initial rotational periods, $P_0 = (900, 1100, 1200, 1400, 1500, 1700)$ s. The dotted lines divide the evolution into three stages according to the value of ω . The red dash-dotted line indicates the equilibrium period $P_{\text{eq}} = 1284.8$ s. The green dashed line indicates the current rotation period of the WD.

The initial angular velocity, Ω_0 , sets the initial fastness parameter in *phase I*: $\omega_0 > 1$ ($\Omega_0 > \Omega_K$; propeller removes angular momentum) or $\omega_0 < 1$ ($\Omega_0 < \Omega_K$; accretion transfers angular momentum). When $\omega \approx 1$ (*phase II*), the accretion and magnetic torques balance, $T_{\text{acc}} \approx T_{\text{mag}}$, so the angular velocity remains constant at the equilibrium value, $\Omega \approx \Omega_{\text{eq}} = \Omega_K$. After the disk is exhausted, the WD evolves in the $\omega < 1$ regime (*phase III*), with only the magnetic dipole exerting torque.

Figures 3 and 4 show the rotation evolution for the two sources, GLEAM-X J1627–5235 and GPM J1839–10, taking into account the initial parameters presented in Table 2 and for $\theta = 90^\circ$. Each phase of evolution described above is identified in this figure. Furthermore, we considered 6 values for the initial rotation period, 3 values below and 3 above the equilibrium period $P_{\text{eq}} = 2\pi/\Omega_{\text{eq}}$. We note that the solution is not sensitive to this initial condition.

The accretion rate adopted in our calculations is $\dot{M} \sim 10^{-7} M_\odot \text{ yr}^{-1}$. This value is not arbitrary: it ensures that the rotational evolution remains consistent with the sources estimated ages. It corresponds to approximately 10% of the Eddington accretion rate and lies within the range expected for double WD mergers. Hydrodynamical simulations of such systems (e.g., Shen, 2015; Schwab et al., 2016; Dan et al., 2014) show that, once the secondary is disrupted, the accretion of the debris disk onto the primary proceeds at near- or super-Eddington rates. Specifically, immediately after the dynamical merger phase, the mass transfer rate can reach $\dot{M} \gtrsim 10^{-5} M_\odot \text{ yr}^{-1}$ (see also Yoon et al., 2007; Becerra et al., 2018). During the subsequent viscous evolution, however, the accretion rate decreases and stabilizes in the range 10^{-5} – $10^{-7} M_\odot \text{ yr}^{-1}$ (Zhang and Jeffery, 2012), consistent with the value required in our model.

Table 2 also presents the parameters derived from the evolution simulation. We observe that the elapsed time required for GPM J1839–10 and GLEAM-X J1627 to reach the current measured period is $\Delta t_{\text{evo}} \approx 0.390$ Gyr and $\Delta t_{\text{evo}} \approx 0.572$ Gyr, respectively. The age for GLEAM-X J1627 agrees with the optical upper limits that predict an age > 0.556 Gyr for a $1.33 M_\odot$ WD. Another interesting parameter worth mentioning is the spindown rate \dot{P}_{evo} at the end of the spin evolution, that is, the \dot{P}_{evo} value that must be observed in the current phase of the source given that only the magnetic torque acts on the star. For the values in Table 2, we infer spindown rates $\sim 10^{-15} \text{ s s}^{-1}$ for both sources.

6. Limiting Magnitudes for WD models

An important way to confirm or rule out the presence of a WD is to look for an optical counterpart that matches the WD’s photospheric emission. Lyman et al. (2025) note that the current deepest upper limit in the *Gaia* *G* band (~ 24.4 mag) for GLEAM-X J1627–5235 lies close to the expected brightness range of WDs at this distance, typically $m_G \sim 22$ – 24 mag. However, as shown in Sec. 4, this limit does not strongly constrain massive WDs, even for ages below 1 Gyr.

To quantify this, Figure 5 shows the cumulative distribution function (CDF) of *Gaia* WDs (all masses) within 200 pc (Genetile Fusillo et al., 2021), with contributions from fainter WDs

corrected for incompleteness following the procedure of Fleury et al. (2022). Specifically, WDs fainter than *Gaia*’s survey limit are not detectable throughout the full 200 pc volume; therefore, each star is weighted by $V_{\text{max}}/V_{\text{lim}}(M_G)$, where $V_{\text{lim}}(M_G)$ is the maximum volume within which WDs of absolute magnitude M_G remain detectable.

This analysis shows that the current limit of $m_G \sim 24.4$ mag corresponds roughly to the 25th percentile of the WD brightness distribution. Reaching the 90th percentile would require sensitivity to $m_G \sim 26.5$ mag, well beyond the current upper limits. Furthermore, GLEAM-X J1627–5235 may host an unusually massive WD. For example, a $1.382 M_\odot$ WD with an age of 750 Myr would have $m_G \sim 28.5$ mag, even fainter than the percentile thresholds. Thus, confirming an WD origin for GLEAM-X J1627–5235 may require optical sensitivities achievable with next-generation telescopes (e.g., ELT and GMT). We note that the estimated age in Sec. 5 depends on the assumed \dot{M} and thus could be adjusted to accommodate a cooler, and hence older, WD if future observations identify one.

For GPM J1839–10, a candidate z_s -band counterpart of 22.7 mag has recently been reported (Pelisoli et al., 2025), although its association remains unconfirmed. If the counterpart is real, whether the system is an isolated WD or a WD+M-dwarf binary (e.g., ILT J1101+5521), the inferred distance of ~ 5.7 kpc is almost certainly overestimated. At such a distance, an optical detection would be highly unlikely with current facilities. This source has $DM = 273.5 \text{ pc cm}^{-3}$, corresponding to $A_G \sim 3.4$ (Hurley-Walker et al., 2023b). Even if the source were an intrinsically bright WD with absolute magnitude $M_G \sim 10$, its apparent magnitude would be $m_G \sim 27$.

For ASKAP J1935+2148, the expected apparent magnitude of a bright WD ($M_G \sim 10$) is $m_G \sim 25$, while for a WD at the 95th percentile of the luminosity distribution ($M_G \sim 15.5$) the expected magnitude is $m_G \sim 30.5$. If this object is a young, bright WD, it may be observable with current telescopes; however, ruling out an isolated WD scenario will require future facilities.

For CHIME J0630+25, its relatively small distance and dispersion measure imply $m_G \sim 22$ even at the 95% confidence level, and thus it should be observable. In this case, as noted by Dong et al. (2025a), establishing a confident association is difficult because the field is crowded and the radio localization is poor, leaving roughly ~ 150 marginal candidates consistent with the position and period. More precise localization is required to confidently identify a counterpart. For DART J1832–0911 and ASKAP J1755–2527, even a bright WD would have expected magnitudes of $m_G \sim 29$ and $m_G \sim 32$, respectively, making it unlikely that their nature can be determined with current optical facilities.

7. Discussion and Conclusion

In a polar cap model context, we showed that the request that isolated LPTs lie above the death line for WD-pulsars requires magnetic fields of a few $\sim 10^9$ G and the presence of small-scale multipolar structure in the magnetosphere (see Section 3). The small-scale multipolar magnetosphere is not merely an

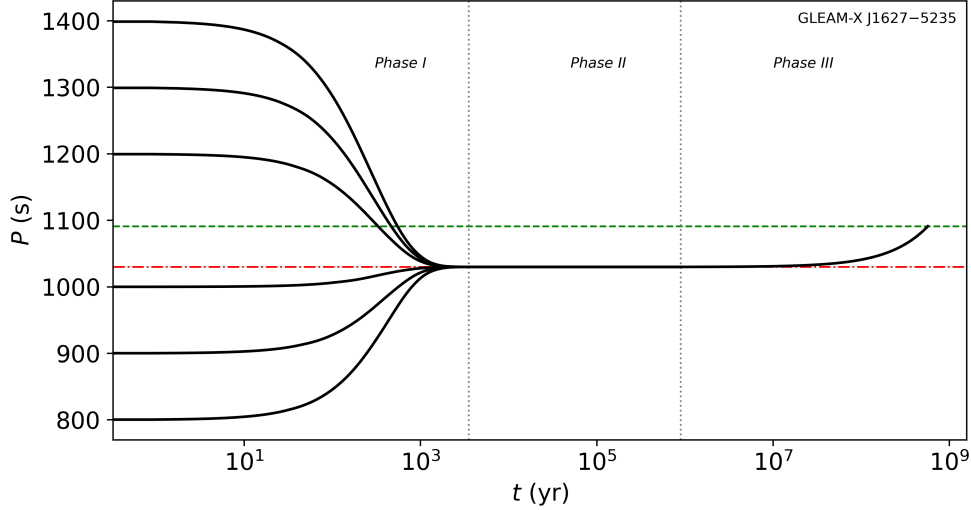


Figure 4: Evolution of the rotation period of GLEAM-X J1627–5235 for an accretion rate of $\dot{M} = 3.35 \times 10^{-7} M_{\odot} \text{ yr}^{-1}$ and for different values of initial rotational periods, $P_0 = (800, 900, 1000, 1200, 1300, 1400)$ s. The dotted lines divide the evolution into three stages according to the value of ω . The red dash-dotted line indicates the equilibrium period $P_{\text{eq}} = 1030.0$ s. The green dashed line indicates the current rotation period of the WD.

auxiliary assumption but a necessary consequence of the merger origin. Differential rotation in the post-merger debris is a robust mechanism for generating non-dipolar surface fields, which are empirically observed in other classes of compact objects. We also include in the analysis a set of observed isolated WDs that are confirmed to be massive, fast-rotating, and highly magnetized. The analysis also suggests the mass ($\sim 1.3 M_{\odot}$) and radius (~ 2500 km) for the LPTs in Table 1, indicating that they are consistent with being made of carbon or oxygen, the most likely compositions for post-merger massive WDs.

We also touched on several pieces of observational evidence of massive and highly magnetized WDs, including the prevalence of WD binaries compared to solar-type main-sequence star binaries. This suggests that a significant fraction of isolated WDs may be double WD merger products. This idea has long been suggested, and the remnants of these mergers can be stable massive WDs, SN Ia, hydrogen-deficient stars (such as R Coronae Borealis stars), or NSs. Recent observations support this hypothesis, with rapidly rotating, strongly magnetized, and massive WDs potentially arising from mergers of WD binaries. Therefore, we have examined the hypothesis that massive WDs can result from merging WD binaries, thereby providing a merger origin for some LPTs. More specifically, it can be an alternative to the WD+M-Dwarf interpretation, specially for objects such as GLEAM-X J1627–5235 that lacks an optical counterpart consistent with the presence of such binary systems. We performed the post-merger spin evolution using a model presented in a previous study (Sousa et al., 2022) for two LPTs, GLEAM-X J1627–5235 and GPM J1839–10, which explains how the stars’ angular momentum changes due to accretion, propeller, and magnetic torques. From the modeling, we inferred the rotational ages of both sources, i.e., the time required for them to reach their currently observed rotational periods. We obtained 572 Myr and 390 Myr for GLEAM-X J1627–5235 and GPM J1839–10, and verified that the upper

limit on their spindown rate is also satisfied (see Section 4 for details).

We also note that this model is consistent with potential X-ray observations, given that accretion episodes from the disk are expected to happen. Borges et al. (2020) noted that a WD accreting matter from the disk can have emission in the soft and hard X-rays, coming from the post-shock region and the hot spots in the WD surface. One of the LPTs present in Table 1, DART J1832-0911, has detected X-ray emission, with a luminosity of $\sim 10^{33} \text{ erg.s}^{-1}$ (Wang et al., 2025). In this case, we can check the expected accretion rate for such luminosity. A good order of magnitude of the accretion rate is GMM/R , and considering the mass and radius of table 1, we find $\sim 10^{-11} M_{\odot}.\text{yr}^{-1}$. This value is consistent with that of other accreting WD classes, such as intermediate polars. Thus, a post-merger WD is consistent with the current paradigm that some, but not all, LPTs exhibit episodic X-ray emission, given that the emission may be linked to the amount of gas remaining in the disk.

Theoretical and observational work on WD pulsars and related areas of physics and astrophysics is flourishing and poised for breakthroughs, given the advanced capabilities of new observational facilities and theoretical advances. Their pulsar-like emission might be observed as magnetar-like activity (see, e.g., Rueda et al., 2013; Coelho et al., 2017; Becerra et al., 2018; Borges et al., 2020, and references therein). An infrared/optical/ultraviolet transient from the cooling of the expanding merger dynamical ejecta peaks a few hours post-merger (Rueda et al., 2022, 2019; Sousa et al., 2023), and is ready for observation by the forthcoming Vera Rubin Observatory at a predicted detection rate of up to 1000 a year (Sousa et al., 2023). Additional multimessenger theoretical predictions involve the emission and possible detection of high-energy neutrinos (Xiao et al., 2016), cosmic rays (Kashiyama et al., 2011; Lobato et al., 2017), gamma-rays (Usov, 1988; Meintjes et al.,

2023; Ikhsanov and Biermann, 2006), and the gravitational waves by merging double WDs, detectable by *LISA*, the Laser Interferometer Space Antenna, (Stroeer and Vecchio, 2006; Korol et al., 2022). *LISA* will possibly measure deviations from pure gravitational-wave-driven orbital dynamics, e.g., given the presence of electromagnetic radiation (Carvalho et al., 2022). Gravitational waves from quadrupole deformations of WD pulsars might also be detected (Sousa et al., 2020, 2024). The Rubin/LSST observing cadence (typically revisiting a given field on timescales of a few days) raises the concern that a fast-evolving, kilonova-like optical transient might be missed or poorly sampled. For the double-WD-merger “kilonova-like” emission considered in Sousa et al. (2023), the optical/IR light curves could remain detectable over multi-day timescales (with the brightest phase lasting of order a few days, followed by a multi-day decline; see the light curves), even with a 2–3 day cadence, for events above the LSST threshold magnitude. Quantitative light-curve examples and estimated upper limits on the LSST detection rate of the expected optical transient from WD-WD mergers have been presented in Sousa et al. (2023). A dedicated discussion of the effects of cadence and the consequent reduction (relative to the upper limits by Sousa et al., 2023) in LSST detection rate of the WD-merger optical transient has recently been presented by M. M. Ridha Fathima et al. (private communication; paper submitted).

In summary, we have provided insights into the properties and origin of LPTs, massive WDs with short rotation periods and strong magnetic fields. Our analysis suggests that the carbon or oxygen abundance is most likely for such WDs, with minor differences in maximum mass and radius. The observations support the hypothesis that these massive WDs can result from WD binary mergers. Recent data and the characteristics of these merged remnants, such as strong magnetism and rapid rotation, further substantiate this. We have highlighted the importance of future optical observations of LPT fields to further constrain and confirm the nature of these objects.

The proposition that LPTs are highly magnetized, fast-rotating WDs formed through double WD mergers broadens our understanding of compact objects. Confirming the isolated WD nature for some LPTs would redefine our understanding of double WD merger outcomes, emphasizing their role not only in Type Ia supernovae but also in producing remnants such as WD pulsars. Future observations using upcoming optical facilities (e.g., ELT and GMT) will be crucial for validating these predictions. Upcoming deep optical searches and future multimessenger observations (e.g., *LISA*) will be decisive in confirming whether LPTs constitute a population of WD pulsars.

Acknowledgments

This work was initiated by Manuel Malheiro and is dedicated to his memory. Manuel was a renowned Brazilian physicist who passed away on June 09, 2024, in São Paulo, Brazil, during the development of this work. He left behind an indelible legacy for the Brazilian nuclear physics and relativistic astrophysics communities that extends beyond scientific knowledge.

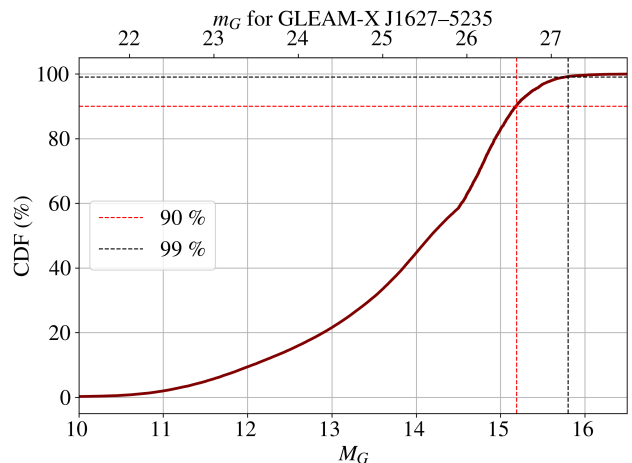


Figure 5: CDF of *Gaia* M_G absolute magnitudes for WDs (bottom x-axis). The top x-axis shows the corresponding apparent G -band magnitudes for GLEAM-X J1627–5235, considering its estimated distance and extinction. The red and black dashed lines mark the magnitudes below which 90% and 99% of the WD population lie, respectively.

The authors thank the referee for the insightful comments. S.V.B. acknowledges support from the NASA ATP program (NNH23ZDA001N-ATP) and the College of Letters and Science at UWM through the Chancellor’s Graduate Student Award and the Research Excellence Award. J.G.C. is grateful for the support of FAPES (1020/2022, 1081/2022, 976/2022, 332/2023), CNPq (311758/2021-5, 306018/2025-0), and FAPESP (grant No. 2021/01089-1). RVL was supported by INCT-FNA (Instituto Nacional de Ciência e Tecnologia, Física Nuclear e Aplicações), research Project No. 464898/2014-5, also thanks CNPq/CAPES, and is very grateful to Professor Manuel Malheiro for his scientific guidance, support, and partnership over several years. M.F.S. thanks FAPESP (2025/05794-2, 2021/01089-1) for the financial support and for the support of CNPq (173535/2023-2). E. Otoniel acknowledges support from FUNCAP(BP6-0241-00335.01.00/25). F.W. is supported through the U.S. National Science Foundation under Grant PHY-2012152.

This work has made use of data from the European Space Agency (ESA) mission *Gaia* (<https://www.cosmos.esa.int/gaia>, Gaia Collaboration et al., 2016, 2023), processed by the *Gaia* Data Processing and Analysis Consortium (DPAC, Babusiaux et al., 2023, <https://www.cosmos.esa.int/web/gaia/dpac/consortium>). Funding for the DPAC has been provided by national institutions, in particular, the institutions participating in the *Gaia* Multilateral Agreement.

Data Availability

The codes used in this study are available from the corresponding author upon reasonable request. All datasets used in this study are publicly available and can be accessed from their original sources:

- WD cooling models: <https://evolgroup.fcaglp.unlp.edu.ar/modelos.html>
- The 3D interstellar extinction map: <https://zenodo.org/records/11394477>
- The *Gaia* white dwarf catalog: https://warwick.ac.uk/fac/sci/physics/research/astro/research/catalogues/gaiaedr3_wd_main.fits.gz

References

- Althaus, L.G., Córscico, A.H., Camisassa, M.E., Torres, S., Gil-Pons, P., Rebassa-Mansergas, A., Raddi, R., 2023. Carbon-oxygen ultra-massive white dwarfs in general relativity. *MNRAS* 523, 4492–4503. doi:10.1093/mnras/stad1720, arXiv:2306.05251.
- Althaus, L.G., García-Berro, E., Isern, J., Córscico, A.H., 2005. Mass-radius relations for massive white dwarf stars. *A&A* 441, 689–694. doi:10.1051/0004-6361:20052996, arXiv:astro-ph/0507559.
- Althaus, L.G., García-Berro, E., Isern, J., Córscico, A.H., Rohrmann, R.D., 2007. The age and colors of massive white dwarf stars. *A&A* 465, 249–255. doi:10.1051/0004-6361:20066059, arXiv:astro-ph/0702024.
- Amorim, L.L., Kepler, S.O., Külebi, B., Jordan, S., Romero, A.D., 2023. Catalog of Magnetic White Dwarfs with Hydrogen Dominated Atmospheres. *ApJ* 944, 56. doi:10.3847/1538-4357/aca6e, arXiv:2301.08862.
- Anumrapudi, A., Kaplan, D.L., Rea, N., Erasmus, N., Kelson, D., Ocker, S.K., Lenc, E., Dobie, D., Hurley-Walker, N., Sivakoff, G., Buckley, D.A.H., Murphy, T., Pritchard, J., Driessen, L., Rose, K., Zic, A., 2025. ASKAP J144834–685644: a newly discovered long period radio transient detected from radio to X-rays. *MNRAS* 542, 1208–1232. doi:10.1093/mnras/staf1227, arXiv:2507.13453.
- Babusiaux, C., Fabricius, C., Khanna, S., Muraveva, T., Reylé, C., Spoto, F., Vallenari, A., Luri, X., Arenou, F., Álvarez, M.A., Anders, F., Antoja, T., Balbinot, E., Barache, C., Bauchet, N., Bossini, D., Busonero, D., Cantat-Gaudin, T., Carrasco, J.M., Dafonte, C., Diakité, S., Figueras, F., Garcia-Gutierrez, A., Garofalo, A., Helmi, A., Jiménez-Arranz, Ó., Jordi, C., Kervella, P., Kostrzewa-Rutkowska, Z., Leclerc, N., Licata, E., Manteiga, M., Masip, A., Monguió, M., Ramos, P., Robichon, N., Robin, A.C., Romero-Gómez, M., Sáez, A., Santoveña, R., Spina, L., Torralba Elipse, G., Weiler, M., 2023. *Gaia* Data Release 3. Catalogue validation. *A&A* 674, A32. doi:10.1051/0004-6361/202243790, arXiv:2206.05989.
- Baumgarte, T.W., Shapiro, S.L., 2024. Could long-period transients be powered by primordial black hole capture? *PhRvD* 109, 063004. doi:10.1103/PhysRevD.109.063004, arXiv:2402.11019.
- Becerra, L., Rueda, J.A., Lorén-Aguilar, P., García-Berro, E., 2018. The Spin Evolution of Fast-rotating, Magnetized Super-Chandrasekhar White Dwarfs in the Aftermath of White Dwarf Mergers. *ApJ* 857, 134. doi:10.3847/1538-4357/aabc12, arXiv:1804.01275.
- Benz, W., Cameron, A.G.W., Press, W.H., Bowers, R.L., 1990. Dynamic mass exchange in doubly degenerate binaries. I - 0.9 and 1.2 solar mass stars. *ApJ* 348, 647–667. doi:10.1086/168273.
- Beskin, V.S., Istomin, A.Y., 2022. Pulsar death line revisited - II. 'The death valley'. *MNRAS* 516, 5084–5091. doi:10.1093/mnras/stac2423, arXiv:2207.04723.
- Beskin, V.S., Litvinov, P.E., 2022. Pulsar death line revisited - I. Almost vacuum gap. *MNRAS* 510, 2572–2582. doi:10.1093/mnras/stab3575, arXiv:2201.02875.
- Bilous, A.V., Watts, A.L., Harding, A.K., Riley, T.E., Arzoumanian, Z., Bogdanov, S., Gendreau, K.C., Ray, P.S., Guillot, S., Ho, W.C.G., Chakrabarty, D., 2019. A NICER View of PSR J0030+0451: Evidence for a Global-scale Multipolar Magnetic Field. *ApJ Lett.* 887, L23. doi:10.3847/2041-8213/ab53e7, arXiv:1912.05704.
- Borges, S.V., 2026. A Correlation between the Final Separation and Mass Ratio from Common-envelope Simulations. *ApJ* 998, 34. doi:10.3847/1538-4357/ae2d53, arXiv:2511.02150.
- Borges, S.V., Rodrigues, C.V., Coelho, J.G., Malheiro, M., Castro, M., 2020. A Magnetic White Dwarf Accretion Model for the Anomalous X-Ray Pulsar 4U 0142+61. *ApJ* 895, 26. doi:10.3847/1538-4357/ab8add, arXiv:2004.07963.
- Buckley, D.A.H., Meintjes, P.J., Potter, S.B., Marsh, T.R., Gänsicke, B.T., 2017. Polarimetric evidence of a white dwarf pulsar in the binary system AR Scorpii. *Nature Astronomy* 1, 0029. doi:10.1038/s41550-016-0029, arXiv:1612.03185.
- Caiazzo, I., Burdge, K.B., Fuller, J., Heyl, J., Kulkarni, S.R., Prince, T.A., Richer, H.B., Schwab, J., Andreoni, I., Bellm, E.C., Drake, A., Duvvuri, D.A., Graham, M.J., Helou, G., Mahabal, A.A., Masci, F.J., Smith, R., Soumagnac, M.T., 2021. A highly magnetized and rapidly rotating white dwarf as small as the Moon. *Nature* 595, 39–42. doi:10.1038/s41586-021-03615-y, arXiv:2107.08458.
- Caleb, M., Lenc, E., Kaplan, D.L., Murphy, T., Men, Y.P., Shannon, R.M., Ferrario, L., Rajwade, K.M., Clarke, T.E., Giacintucci, S., Hurley-Walker, N., Hyman, S.D., Lower, M.E., McSweeney, S., Ravi, V., Barr, E.D., Buchner, S., Flynn, C.M.L., Hessels, J.W.T., Kramer, M., Pritchard, J., Stappers, B.W., 2024. An emission-state-switching radio transient with a 54-minute period. *Nature Astronomy* 8, 1159–1168. doi:10.1038/s41550-024-02277-w, arXiv:2407.12266.

- Camisassa, M.E., Althaus, L.G., Córscico, A.H., De Gerónimo, F.C., Miller Bertolami, M.M., Novarino, M.L., Rohrmann, R.D., Wachlin, F.C., García-Berro, E., 2019. The evolution of ultra-massive white dwarfs. *A&A* 625, A87. doi:10.1051/0004-6361/201833822, arXiv:1807.03894.
- Camisassa, M.E., Althaus, L.G., Koester, D., Torres, S., Gil-Pons, P., Córscico, A.H., 2022. The evolution of ultra-massive carbon-oxygen white dwarfs. *MNRAS* 511, 5198–5206. doi:10.1093/mnras/stac348, arXiv:2202.03495.
- Cardelli, J.A., Clayton, G.C., Mathis, J.S., 1989. The Relationship between Infrared, Optical, and Ultraviolet Extinction. *ApJ* 345, 245. doi:10.1086/167900.
- Carvalho, G.A., Anjos, R.C.d., Coelho, J.G., Lobato, R.V., Malheiro, M., Marinho, R.M., Rodriguez, J.F., Rueda, J.A., Ruffini, R., 2022. Orbital Decay of Double White Dwarfs: Beyond Gravitational-wave Radiation Effects. *ApJ* 940, 90. doi:10.3847/1538-4357/ac9841, arXiv:2208.00863.
- Castro-Tapia, M., Camisassa, M., Zhang, S., 2026. Evolution of a Long-lived Deep-seated Main-sequence Magnetic Field during White Dwarf Cooling. *The Astrophysical Journal* 998, 28. doi:10.3847/1538-4357/ae2fb6.
- Cerutti, B., Philippov, A.A., Spitkovsky, A., 2016. Modelling high-energy pulsar light curves from first principles. *MNRAS* 457, 2401–2414. doi:10.1093/mnras/stw124, arXiv:1511.01785.
- Chen, K., Ruderman, M., 1993. Pulsar death lines and death valley. *The Astrophysical Journal* 402, 264–270. doi:10.1086/172129.
- Cheng, S., Cummings, J.D., Ménard, B., Toonen, S., 2020. Double White Dwarf Merger Products among High-mass White Dwarfs. *ApJ* 891, 160. doi:10.3847/1538-4357/ab733c, arXiv:1910.09558.
- Coelho, J.G., Cáceres, D.L., de Lima, R.C.R., Malheiro, M., Rueda, J.A., Ruffini, R., 2017. The rotation-powered nature of some soft gamma-ray repeaters and anomalous X-ray pulsars. *A&A* 599, A87. doi:10.1051/0004-6361/201629521.
- Coelho, J.G., de Araujo, J.C.N., Ladislau, S.M., Nunes, R.C., 2021. Observational Constraints on the Pulsar Wind Model: The Cases of Crab and Vela. *ApJ* 920, 57. doi:10.3847/1538-4357/ac1d41, arXiv:2105.11957.
- Curd, B., Gianninas, A., Bell, K.J., Kilic, M., Romero, A.D., Allende Prieto, C., Winget, D.E., Winget, K.I., 2017. Four new massive pulsating white dwarfs including an ultramassive DAV. *MNRAS* 468, 239–249. doi:10.1093/mnras/stx320, arXiv:1702.03343.
- Dan, M., Rosswog, S., Brüggen, M., Podsiadlowski, P., 2014. The structure and fate of white dwarf merger remnants. *MNRAS* 438, 14–34. doi:10.1093/mnras/stt1766, arXiv:1308.1667.
- de Lima, R.C.R., Coelho, J.G., Pereira, J.P., Rodrigues, C.V., Rueda, J.A., 2020. Evidence for a Multipolar Magnetic Field in SGR J1745-2900 from X-Ray Light-curve Analysis. *ApJ* 889, 165. doi:10.3847/1538-4357/ab65f4, arXiv:1912.12336.
- de Lima, R.C.R., Pereira, J.P., Coelho, J.G., Nunes, R.C., Stecchini, P.E., Castro, M., Gomes, P., da Silva, R.R., Rodrigues, C.V., de Araujo, J.C.N., Bejger, M., Haensel, P., Zdunik, J.L., 2024. Evidence for 3XMM J185246.6+003317 as a massive magnetar with a low magnetic field. *Journal of High Energy Astrophysics* 42, 52–62. doi:10.1016/j.jheap.2024.04.001, arXiv:2210.06648.
- de Ruiter, I., Rajwade, K.M., Bassa, C.G., Rowlinson, A., Wijers, R.A.M.J., Kilpatrick, C.D., Stefansson, G., Callingham, J.R., Hessels, J.W.T., Clarke, T.E., Peters, W., Wijnands, R.A.D., Shimwell, T.W., ter Veen, S., Morello, V., Zeimann, G.R., Mahadevan, S., 2025. Sporadic radio pulses from a white dwarf binary at the orbital period. *Nature Astronomy* 9, 672–684. doi:10.1038/s41550-025-02491-0, arXiv:2408.11536.
- Dobie, D., Zic, A., Oswald, L.S., Pritchard, J., Lower, M.E., Wang, Z., Qiu, H., Hurley-Walker, N., Wang, Y., Lenc, E., Kaplan, D.L., Anumarlapudi, A., Auchettl, K., Bailes, M., Cameron, A.D., Cooke, J., Deller, A., Driessen, L.N., Freeburn, J., Murphy, T., Shannon, R.M., Stewart, A.J., 2024. A two-minute burst of highly polarized radio emission originating from low Galactic latitude. *MNRAS* 535, 909–923. doi:10.1093/mnras/stae2376, arXiv:2406.12352.
- Dong, F.A., Clarke, T.E., Curtin, A., Kumar, A., Mckinven, R., Shin, K., Stairs, I., Brar, C., Burdge, K., Chatterjee, S., Cook, A.M., Fonseca, E., Gaensler, B.M., Hessels, J.W., Kaspi, V.M., Lazda, M., Main, R., Masui, K.W., McKee, J.W., Meyers, B.W., Pearlman, A.B., Ransom, S.M., Scholz, P., Smith, K.M., Tan, C.M., 2025a. CHIME/Fast Radio Burst/Pulsar Discovery of a Nearby Long-period Radio Transient with a Timing Glitch. *ApJ Lett.* 990, L49. doi:10.3847/2041-8213/adfa8e, arXiv:2407.07480.
- Dong, F.A., E Clarke, T., Curtin, A., Kumar, A., Mckinven, R., Shin, K., Stairs, I., Brar, C., Burdge, K., Chatterjee, S., Cook, A.M., Fonseca, E., Gaensler, B.M., Hessels, J.W., Kaspi, V.M., Lazda, M., Main, R., Masui, K.W., McKee, J.W., Meyers, B.W., Pearlman, A.B., Ransom, S.M., Scholz, P., Smith, K.M., Tan, C.M., 2024. CHIME/FRB/Pulsar discovery of a nearby long period radio transient with a timing glitch. arXiv e-prints, arXiv:2407.07480doi:10.48550/arXiv.2407.07480, arXiv:2407.07480.
- Dong, F.A., Shin, K., Law, C., Ng, M., Stairs, I., Bower, G., Cassity, A., Fonseca, E., Gaensler, B.M., Hessels, J.W.T., Kaspi, V.M., Kharel, B., Leung, C., Main, R.A., Masui, K.W., McKee, J.W., Meyers, B.W., Modilim, O., Pandhi, A., Pearlman, A.B., Ransom, S.M., Scholz, P., Smith, K., 2025b. CHIME/Fast Radio Burst Discovery of an Unusual Circularly Polarized Long-period Radio Transient with an

Accelerating Spin Period. *ApJ Lett.* 988, L29. doi:10.3847/2041-8213/adeaab, arXiv:2507.05139.

du Plessis, L., Venter, C., Wadiasingh, Z., Harding, A.K., Buckley, D.A.H., Potter, S.B., Meintjes, P.J., 2022. Probing the non-thermal emission geometry of AR Sco via optical phase-resolved polarimetry. *MNRAS* 510, 2998–3010. doi:10.1093/mnras/stab3595, arXiv:2112.08708.

Ferrario, L., de Martino, D., Gänsicke, B.T., 2015. Magnetic White Dwarfs. *Space Science Reviews* 191, 111–169. doi:10.1007/s11214-015-0152-0, arXiv:1504.08072.

Ferrario, L., Vennes, S., Wickramasinghe, D.T., Bailey, J.A., Christian, D.J., 1997. EUVE J0317-855: a rapidly rotating, high-field magnetic white dwarf. *MNRAS* 292, 205–217. doi:10.1093/mnras/292.2.205.

Fleury, L., Caiazzo, I., Heyl, J., 2022. The cooling of massive white dwarfs from Gaia EDR3. *MNRAS* 511, 5984–5993. doi:10.1093/mnras/stac458, arXiv:2110.00598.

Gaia Collaboration, Prusti, T., de Bruijne, J.H.J., Brown, A.G.A., Vallenari, A., Babusiaux, C., Bailer-Jones, C.A.L., Bastian, U., Biermann, M., Evans, D.W., Eyer, L., Jansen, F., Jordi, C., Klioner, S.A., Lammers, U., Lindegren, L., Luri, X., Mignard, F., Milligan, D.J., Panem, C., Poinsignon, V., Pourbaix, D., Randich, S., Sarri, G., Sartoretti, P., Siddiqui, H.I., Soubiran, C., Valette, V., van Leeuwen, F., Walton, N.A., Aerts, C., Arenou, F., Cropper, M., Drimmel, R., Høg, E., Katz, D., Lattanzi, M.G., O’Mullane, W., Grebel, E.K., Holland, A.D., Huc, C., Passot, X., Bramante, L., Cacciari, C., Castañeda, J., Chaoul, L., Cheek, N., De Angeli, F., Fabricius, C., Guerra, R., Hernández, J., Jean-Antoine-Piccolo, A., Masana, E., Messineo, R., Mowlavi, N., Nienartowicz, K., Ordóñez-Blanco, D., Panuzzo, P., Portell, J., Richards, P.J., Riello, M., Seabroke, G.M., Tanga, P., Thévenin, F., Torra, J., Els, S.G., Gracia-Abril, G., Comoretto, G., Garcia-Reinaldos, M., Lock, T., Mercier, E., Altmann, M., Andrae, R., Astraatmadja, T.L., Bellas-Velidis, I., Benson, K., Berthier, J., Blomme, R., Busso, G., Carry, B., Cellino, A., Clementini, G., Cowell, S., Creevey, O., Cuypers, J., Davidson, M., De Ridder, J., de Torres, A., Delchambre, L., Dell’Oro, A., Ducourant, C., Frémat, Y., García-Torres, M., Gosset, E., Halbwachs, J.L., Hambly, N.C., Harrison, D.L., Hauser, M., Hestroffer, D., Hodgkin, S.T., Huckle, H.E., Hutton, A., Jasiewicz, G., Jordan, S., Kontizas, M., Korn, A.J., Lanzafame, A.C., Manteiga, M., Moitinho, A., Muinonen, K., Osinde, J., Pancino, E., Pauwels, T., Petit, J.M., Recio-Blanco, A., Robin, A.C., Sarro, L.M., Siopis, C., Smith, M., Smith, K.W., Sozzetti, A., Thuillot, W., van Reeven, W., Viala, Y., Abbas, U., Abreu Aramburu, A., Accart, S., Aguado, J.J., Allan, P.M., Allasia, W., Altavilla, G., Álvarez, M.A., Alves, J., Anderson, R.I., Andrei, A.H., Anglada Varela, E., Antiche, E., Antoja, T., Antón, S., Arcay, B., Atzei, A., Ayache, L., Bach, N., Baker, S.G., Balaguer-Núñez, L., Barache, C., Barata,

C., Barbier, A., Barblan, F., Baroni, M., Barrado y Navascués, D., Barros, M., Barstow, M.A., Becciani, U., Bellazzini, M., Bellei, G., Bello García, A., Belokurov, V., Bendjoya, P., Berihuete, A., Bianchi, L., Bienaymé, O., Billebaud, F., Blagorodnova, N., Blanco-Cuaresma, S., Boch, T., Bombrun, A., Borrachero, R., Bouquillon, S., Bourda, G., Bouy, H., Bragaglia, A., Breddels, M.A., Brouillet, N., Brüsemeister, T., Bucciarelli, B., Budnik, F., Burgess, P., Burgon, R., Burlacu, A., Busonero, D., Buzzzi, R., Caffau, E., Cambras, J., Campbell, H., Cancelliere, R., Cantat-Gaudin, T., Carlucci, T., Carrasco, J.M., Castellani, M., Charlot, P., Charnas, J., Charvet, P., Chassat, F., Chiavassa, A., Clotet, M., Cocozza, G., Collins, R.S., Collins, P., Costigan, G., 2016. The Gaia mission. *A&A* 595, A1. doi:10.1051/0004-6361/201629272, arXiv:1609.04153.

Gaia Collaboration, Vallenari, A., Brown, A.G.A., Prusti, T., de Bruijne, J.H.J., Arenou, F., Babusiaux, C., Biermann, M., Creevey, O.L., Ducourant, C., Evans, D.W., Eyer, L., Guerra, R., Hutton, A., Jordi, C., Klioner, S.A., Lammers, U.L., Lindegren, L., Luri, X., Mignard, F., Panem, C., Pourbaix, D., Randich, S., Sartoretti, P., Soubiran, C., Tanga, P., Walton, N.A., Bailer-Jones, C.A.L., Bastian, U., Drimmel, R., Jansen, F., Katz, D., Lattanzi, M.G., van Leeuwen, F., Bakker, J., Cacciari, C., Castañeda, J., De Angeli, F., Fabricius, C., Fouesneau, M., Frémat, Y., Galluccio, L., Guerrier, A., Heiter, U., Masana, E., Messineo, R., Mowlavi, N., Nicolas, C., Nienartowicz, K., Pailler, F., Panuzzo, P., Riclet, F., Roux, W., Seabroke, G.M., Sordo, R., Thévenin, F., Gracia-Abril, G., Portell, J., Teyssier, D., Altmann, M., Andrae, R., Audard, M., Bellas-Velidis, I., Benson, K., Berthier, J., Blomme, R., Burgess, P.W., Busonero, D., Busso, G., Cánovas, H., Carry, B., Cellino, A., Cheek, N., Clementini, G., Damerdj, Y., Davidson, M., de Teodoro, P., Nuñez Campos, M., Delchambre, L., Dell’Oro, A., Esquej, P., Fernández-Hernández, J., Fraile, E., Garabato, D., García-Lario, P., Gosset, E., Haigron, R., Halbwachs, J.L., Hambly, N.C., Harrison, D.L., Hernández, J., Hestroffer, D., Hodgkin, S.T., Holl, B., Janßen, K., Jevardat de Fombelle, G., Jordan, S., Krone-Martins, A., Lanzafame, A.C., Löffler, W., Marchal, O., Marrese, P.M., Moitinho, A., Muinonen, K., Osborne, P., Pancino, E., Pauwels, T., Recio-Blanco, A., Reylé, C., Riello, M., Rimoldini, L., Roegiers, T., Rybizki, J., Sarro, L.M., Siopis, C., Smith, M., Sozzetti, A., Utrilla, E., van Leeuwen, M., Abbas, U., Abraham, P., Abreu Aramburu, A., Aerts, C., Aguado, J.J., Ajaj, M., Aldea-Montero, F., Altavilla, G., Álvarez, M.A., Alves, J., Anders, F., Anderson, R.I., Anglada Varela, E., Antoja, T., Baines, D., Baker, S.G., Balaguer-Núñez, L., Balbinot, E., Balog, Z., Barache, C., Barbato, D., Barros, M., Barstow, M.A., Bartolomé, S., Bassilana, J.L., Bauchet, N., Becciani, U., Bellazzini, M., Berihuete, A., Bernet, M., Bertone, S., Bianchi, L., Binnenfeld, A., Blanco-Cuaresma, S., Blazere, A., Boch, T., Bombrun, A., Bossini, D., Bouquillon, S., Bragaglia, A., Bramante, L., Breedt, E., Bressan, A., Brouillet, N., Brugaletta, E., Bucciarelli, B., Burlacu, A., Butkevich, A.G., Buzzzi, R., Caffau, E., Cancelliere, R., Cantat-Gaudin, T.,

- Carballo, R., Carlucci, T., Carnerero, M.I., Carrasco, J.M., Casamiquela, L., Castellani, M., Castro-Ginard, A., Chaoul, L., Charlot, P., Chemin, L., Chiamanda, V., Chiavassa, A., Chornay, N., Comoretto, G., Contursi, G., Cooper, W.J., Cornez, T., Cowell, S., Crifo, F., Cropper, M., Crosta, M., Crowley, C., Dafonte, C., Dapergolas, A., David, M., David, P., de Laverny, P., De Luise, F., De March, R., 2023. Gaia Data Release 3. Summary of the content and survey properties. *A&A* 674, A1. doi:10.1051/0004-6361/202243940, arXiv:2208.00211.
- Gänsicke, B.T., Rodríguez-Gil, P., Gentile Fusillo, N.P., Inight, K., Schreiber, M.R., Pala, A.F., Tremblay, P.E., 2020. Single magnetic white dwarfs with Balmer emission lines: a small class with consistent physical characteristics as possible signposts for close-in planetary companions. *MNRAS* 499, 2564–2574. doi:10.1093/mnras/staa2969, arXiv:2009.11925.
- García-Berro, E., Lorén-Aguilar, P., Aznar-Siguán, G., Torres, S., Camacho, J., Althaus, L.G., Córscico, A.H., Külebi, B., Isern, J., 2012. Double Degenerate Mergers as Progenitors of High-field Magnetic White Dwarfs. *ApJ* 749, 25. doi:10.1088/0004-637X/749/1/25.
- Geng, J.J., Zhang, B., Huang, Y.F., 2016. A Model of White Dwarf Pulsar AR Scorpii. *ApJ Lett.* 831, L10. doi:10.3847/2041-8205/831/1/L10, arXiv:1609.02508.
- Gentile Fusillo, N.P., Tremblay, P.E., Cukanovaite, E., Vorontseva, A., Lallement, R., Hollands, M., Gänsicke, B.T., Burdge, K.B., McCleery, J., Jordan, S., 2021. A catalogue of white dwarfs in Gaia EDR3. *MNRAS* 508, 3877–3896. doi:10.1093/mnras/stab2672, arXiv:2106.07669.
- Gentile Fusillo, N.P., Tremblay, P.E., Gänsicke, B.T., Manser, C.J., Cunningham, T., Cukanovaite, E., Hollands, M., Marsh, T., Raddi, R., Jordan, S., Toonen, S., Geier, S., Barstow, M., Cummings, J.D., 2018. A Gaia Data Release 2 catalogue of white dwarfs and a comparison with SDSS. *Monthly Notices of the Royal Astronomical Society* 482, 4570–4591. URL: <https://doi.org/10.1093/mnras/sty3016>, doi:10.1093/mnras/sty3016.
- Gil, J., Mitra, D., 2001. Vacuum Gaps in Pulsars and PSR J2144–3933. *The Astrophysical Journal* 550, 383. doi:10.1086/319714, arXiv:astro-ph/0010603.
- Glanz, H., Perets, H.B., 2021. Simulations of common envelope evolution in triple systems: circumstellar case. *MNRAS* 500, 1921–1932. doi:10.1093/mnras/staa3242, arXiv:2004.00020.
- Goldreich, P., Julian, W.H., 1969. Pulsar Electrodynamics. *The Astrophysical Journal* 157, 869. doi:10.1086/150119.
- Guerrero, J., García-Berro, E., Isern, J., 2004. Smoothed Particle Hydrodynamics simulations of merging white dwarfs. *A&A* 413, 257–272. doi:10.1051/0004-6361:20031504.
- Guo, J., Wang, X., Liu, Q., Filippenko, A.V., Brink, T.G., Zhao, J., Zhang, W., Yang, Y., Lin, J., Peng, H., Chen, H., Mirzakholov, D.O., Ehgamberdiev, S.A., Ma, B., Mo, J., Liu, C., Xi, G., Jiang, X., Xiang, D., Zhang, J., 2026. A Highly Magnetic Ultramassive White Dwarf with a 23 minute Rotation Period. *ApJ* 998, 292. doi:10.3847/1538-4357/ae3a7a, arXiv:2601.10188.
- Harding, A.K., Muslimov, A.G., 2011. Pulsar Pair Cascades in a Distorted Magnetic Dipole Field. *ApJ Lett.* 726, L10. doi:10.1088/2041-8205/726/1/L10, arXiv:1012.0451.
- He, C., Ng, C.Y., Kaspi, V.M., 2013. The Correlation between Dispersion Measure and X-Ray Column Density from Radio Pulsars. *ApJ* 768, 64. doi:10.1088/0004-637X/768/1/64, arXiv:1303.5170.
- Heber, U., 2009. Hot Subdwarf Stars. *Annual Review of Astronomy and Astrophysics* 47, 211–251. doi:10.1146/annurev-astro-082708-101836.
- Hermes, J.J., Kepler, S.O., Castanheira, B.G., Gianninas, A., Winget, D.E., Montgomery, M.H., Brown, W.R., Harrold, S.T., 2013. Discovery of an Ultramassive Pulsating White Dwarf. *ApJ Lett.* 771, L2. doi:10.1088/2041-8205/771/1/L2, arXiv:1306.4024.
- Hewish, A., Bell, S.J., Pilkington, J.D.H., Scott, P.F., Collins, R.A., 1968. Observation of a Rapidly Pulsating Radio Source. *Nature* 217, 709–713. doi:10.1038/217709a0.
- Hollands, M.A., Tremblay, P.E., Gänsicke, B.T., Camisassa, M.E., Koester, D., Aungwerojwit, A., Chote, P., Córscico, A.H., Dhillon, V.S., Gentile-Fusillo, N.P., Hoskin, M.J., Izquierdo, P., Marsh, T.R., Steeghs, D., 2020. An ultramassive white dwarf with a mixed hydrogen-carbon atmosphere as a likely merger remnant. *Nature Astronomy* 4, 663–669. doi:10.1038/s41550-020-1028-0, arXiv:2003.00028.
- Horváth, C., Rea, N., Hurley-Walker, N., McSweeney, S.J., Perley, R.A., Lenc, E., 2025. A binary model of long period radio transients and white dwarf pulsars. arXiv e-prints, arXiv:2507.15352doi:10.48550/arXiv.2507.15352, arXiv:2507.15352.
- Hurley-Walker, N., McSweeney, S.J., Bahramian, A., Rea, N., Horváth, C., Buchner, S., Williams, A., Meyers, B.W., Strader, J., Aydi, E., Urquhart, R., Chomiuk, L., Galvin, T.J., Coti Zelati, F., Bailes, M., 2024. A 2.9 hr Periodic Radio Transient with an Optical Counterpart. *ApJ Lett.* 976, L21. doi:10.3847/2041-8213/ad890e, arXiv:2408.15757.
- Hurley-Walker, N., Rea, N., McSweeney, S.J., Meyers, B.W., Lenc, E., Heywood, I., Hyman, S.D., Men, Y.P., Clarke, T.E., Coti Zelati, F., Price, D.C., Horváth, C., Galvin, T.J., Anderson, G.E., Bahramian, A., Barr, E.D., Bhat, N.D.R., Caleb, M., Dall’Ora, M., de Martino, D., Giacintucci, S., Morgan, J.S., Rajwade, K.M., Stappers, B., Williams, A., 2023a. A

- long-period radio transient active for three decades. *Nature* 619, 487–490. doi:10.1038/s41586-023-06202-5.
- Hurley-Walker, N., Rea, N., McSweeney, S.J., Meyers, B.W., Lenc, E., Heywood, I., Hyman, S.D., Men, Y.P., Clarke, T.E., Coti Zelati, F., Price, D.C., Horváth, C., Galvin, T.J., Anderson, G.E., Bahramian, A., Barr, E.D., Bhat, N.D.R., Caleb, M., Dall’Ora, M., de Martino, D., Giacintucci, S., Morgan, J.S., Rajwade, K.M., Stappers, B., Williams, A., 2023b. A long-period radio transient active for three decades. *Nature* 619, 487–490. doi:10.1038/s41586-023-06202-5.
- Hurley-Walker, N., Zhang, X., Bahramian, A., McSweeney, S.J., O’Doherty, T.N., Hancock, P.J., Morgan, J.S., Anderson, G.E., Heald, G.H., Galvin, T.J., 2022a. A radio transient with unusually slow periodic emission. *Nature* 601, 526–530. doi:10.1038/s41586-021-04272-x.
- Hurley-Walker, N., Zhang, X., Bahramian, A., McSweeney, S.J., O’Doherty, T.N., Hancock, P.J., Morgan, J.S., Anderson, G.E., Heald, G.H., Galvin, T.J., 2022b. A radio transient with unusually slow periodic emission. *Nature* 601, 526–530. doi:10.1038/s41586-021-04272-x.
- Hyman, S.D., Lazio, T.J.W., Kassim, N.E., Ray, P.S., Markwardt, C.B., Yusef-Zadeh, F., 2005. A powerful bursting radio source towards the Galactic Centre. *Nature* 434, 50–52. doi:10.1038/nature03400, arXiv:astro-ph/0503052.
- Iaconi, R., De Marco, O., 2019. Speaking with one voice: simulations and observations discuss the common envelope α parameter. *MNRAS* 490, 2550–2566. doi:10.1093/mnras/stz2756, arXiv:1902.02039.
- Ikhsanov, N.R., Biermann, P.L., 2006. High-energy emission of fast rotating white dwarfs. *A&A* 445, 305–312. doi:10.1051/0004-6361:20053179, arXiv:astro-ph/0509070.
- Ivanova, N., Justham, S., Ricker, P., 2020. Common Envelope Evolution. doi:10.1088/2514-3433/abb6f0.
- Jiménez-Esteban, F.M., Torres, S., Rebassa-Mansergas, A., Skorobogatov, G., Solano, E., Cantero, C., Rodrigo, C., 2018. A white dwarf catalogue from Gaia-DR2 and the Virtual Observatory. *MNRAS* 480, 4505–4518. doi:10.1093/mnras/sty2120, arXiv:1807.02559.
- Kashiyama, K., Ioka, K., Kawanaka, N., 2011. White dwarf pulsars as possible cosmic ray electron-positron factories. *PhRvD* 83, 023002. doi:10.1103/PhysRevD.83.023002, arXiv:1009.1141.
- Kaspi, V.M., 2023. Slow-beating radio waves from a long-lived source. *Nature* 619, 472–473. doi:10.1038/d41586-023-02295-0.
- Katz, J.I., 2022. GLEAM-X J162759.5–523504.3 as a white dwarf pulsar. *APSS* 367, 108. doi:10.1007/s10509-022-04146-2, arXiv:2203.08112.
- Kepler, S.O., Pelisoli, I., Jordan, S., Kleinman, S.J., Koester, D., Külebi, B., Peçanha, V., Castanheira, B.G., Nitta, A., Costa, J.E.S., Winget, D.E., Kanaan, A., Fraga, L., 2013. Magnetic white dwarf stars in the Sloan Digital Sky Survey. *Monthly Notices of the Royal Astronomical Society* 429, 2934. doi:10.1093/mnras/sts522, arXiv:1211.5709.
- Kepler, S.O., Pelisoli, I., Koester, D., Ourique, G., Kleinman, S.J., Romero, A.D., Nitta, A., Eisenstein, D.J., Costa, J.E.S., Külebi, B., Jordan, S., Dufour, P., Giommi, P., Rebassa-Mansergas, A., 2015. New white dwarf stars in the Sloan Digital Sky Survey Data Release 10. *MNRAS* 446, 4078–4087. doi:10.1093/mnras/stu2388, arXiv:1411.4149.
- Kepler, S.O., Pelisoli, I., Koester, D., Ourique, G., Romero, A.D., Reindl, N., Kleinman, S.J., Eisenstein, D.J., Valois, A.D.M., Amaral, L.A., 2016. New white dwarf and subdwarf stars in the Sloan Digital Sky Survey Data Release 12. *MNRAS* 455, 3413–3423. doi:10.1093/mnras/stv2526, arXiv:1510.08409.
- Kilic, M., Bergeron, P., Blouin, S., Bédard, A., 2021a. The most massive white dwarfs in the solar neighbourhood. *MNRAS* 503, 5397–5408. doi:10.1093/mnras/stab767, arXiv:2103.06906.
- Kilic, M., Kosakowski, A., Moss, A.G., Bergeron, P., Conly, A.A., 2021b. An Isolated White Dwarf with a 70 s Spin Period. *ApJ Lett.* 923, L6. doi:10.3847/2041-8213/ac3b60, arXiv:2111.14902.
- Kilic, M., Moss, A.G., Kosakowski, A., Bergeron, P., Conly, A.A., Brown, W.R., Toonen, S., Williams, K.A., Dufour, P., 2023. The merger fraction of ultramassive white dwarfs. *Monthly Notices of the Royal Astronomical Society* 518, 2341–2353.
- Korol, V., Hallakoun, N., Toonen, S., Karnesis, N., 2022. Observationally driven Galactic double white dwarf population for LISA. *Mon. Not. R. Astron. Soc.* 511, 5936–5947. doi:10.1093/mnras/stac415.
- Kuelebi, B., Jordan, S., Euchner, F., Gaensicke, B.T., Hirsch, H., 2010. VizieR Online Data Catalog: Magnetic fields in white dwarfs (Kuelebi+, 2009). *VizieR Online Data Catalog*, J/A+A/506/1341.
- Külebi, B., Jordan, S., Euchner, F., Gänsicke, B.T., Hirsch, H., 2009. Analysis of hydrogen-rich magnetic white dwarfs detected in the Sloan Digital Sky Survey. *A&A* 506, 1341–1350. doi:10.1051/0004-6361/200912570, arXiv:0907.2372.
- Külebi, B., Jordan, S., Nelan, E., Bastian, U., Altmann, M., 2010. Constraints on the origin of the massive, hot, and rapidly rotating magnetic white dwarf RE J 0317-853 from an HST parallax measurement. *A&A* 524, A36. doi:10.1051/0004-6361/201015237, arXiv:1007.4978.

- Lee, Y.W.J., Caleb, M., Murphy, T., Lenc, E., Kaplan, D.L., Ferrario, L., Wadiasingh, Z., Anumarlapudi, A., Hurley-Walker, N., Karambelkar, V., Ocker, S.K., McSweeney, S., Qiu, H., Rajwade, K.M., Zic, A., Bannister, K.W., Bhat, N.D.R., Deller, A., Dobie, D., Driessen, L.N., Gendreau, K., Glowacki, M., Gupta, V., Jahns-Schindler, J.N., Jaini, A., James, C.W., Kasliwal, M.M., Lower, M.E., Shannon, R.M., Uttarkar, P.A., Wang, Y., Wang, Z., 2025. The emission of interpulses by a 6.45-h-period coherent radio transient. *Nature Astronomy* 9, 393–405. doi:10.1038/s41550-024-02452-z, arXiv:2501.09133.
- Lobato, R.V., Coelho, J.G., Malheiro, M., 2017. Ultra-high energy cosmic rays from white dwarf pulsars and the Hillas criterion, in: *Journal of Physics Conference Series*, p. 012005. doi:10.1088/1742-6596/861/1/012005, arXiv:1703.06208.
- Lockhart, W., Gralla, S.E., Özel, F., Psaltis, D., 2019. X-ray light curves from realistic polar cap models: Inclined pulsar magnetospheres and multipole fields. *Monthly Notices of the Royal Astronomical Society* 490, 1774–1783. doi:10.1093/mnras/stz2524, arXiv:1904.11534.
- Loeb, A., Maoz, D., 2022. A Hot Subdwarf Model for the 18.18 minutes Pulsar GLEAM-X. *Research Notes of the American Astronomical Society* 6, 27. doi:10.3847/2515-5172/ac52f1, arXiv:2202.04949.
- Longland, R., Lorén-Aguilar, P., José, J., García-Berro, E., Althaus, L.G., 2012. Lithium production in the merging of white dwarf stars. *A&A* 542, A117. doi:10.1051/0004-6361/201219289, arXiv:1205.2538.
- Lopes de Oliveira, R., Bruch, A., Rodrigues, C.V., Oliveira, A.S., Mukai, K., 2020. CTCV J2056-3014: An X-Ray-faint Intermediate Polar Harboring an Extremely Fast-spinning White Dwarf. *ApJ Lett.* 898, L40. doi:10.3847/2041-8213/aba618.
- Lorén-Aguilar, P., Isern, J., García-Berro, E., 2009. High-resolution smoothed particle hydrodynamics simulations of the merger of binary white dwarfs. *A&A* 500, 1193–1205. doi:10.1051/0004-6361/200811060.
- Lyman, J.D., Dhillon, V.S., Kamann, S., Chrimes, A.A., Levan, A.J., Pelisoli, I., Steeghs, D.T.H., Wiersema, K., 2025. Constraints on optical and near-infrared variability in the localization of the long-period radio transient GLEAM-X J1627-52. *MNRAS* 538, 925–942. doi:10.1093/mnras/staf325, arXiv:2502.14688.
- Maoz, D., Hallakoun, N., 2017. The binary fraction, separation distribution, and merger rate of white dwarfs from SPY. *MNRAS* 467, 1414–1425. doi:10.1093/mnras/stx102, arXiv:1609.02156.
- Maoz, D., Hallakoun, N., Badenes, C., 2018. The separation distribution and merger rate of double white dwarfs: improved constraints. *MNRAS* 476, 2584–2590. doi:10.1093/mnras/sty339, arXiv:1801.04275.
- Marsh, T.R., Gänsicke, B.T., Hümmerich, S., Hamsch, F.J., Bernhard, K., Lloyd, C., Breedt, E., Stanway, E.R., Steeghs, D.T., Parsons, S.G., Toloza, O., Schreiber, M.R., Jonker, P.G., van Roestel, J., Kupfer, T., Pala, A.F., Dhillon, V.S., Hardy, L.K., Littlefair, S.P., Aungwerojwit, A., Arjyotha, S., Koester, D., Bochinski, J.J., Haswell, C.A., Frank, P., Wheatley, P.J., 2016. A radio-pulsing white dwarf binary star. *Nature* 537, 374–377. doi:10.1038/nature18620, arXiv:1607.08265.
- Meintjes, P.J., Madzime, S.T., Kaplan, Q., van Heerden, H.J., 2023. Spun-Up Rotation-Powered Magnetized White Dwarfs in Close Binaries as Possible Gamma-ray Sources: Signatures of Pulsed Modulation from AE Aquarii and AR Scorpii in Fermi-LAT Data. *Galaxies* 11, 14. doi:10.3390/galaxies11010014.
- Menou, K., Esin, A.A., Narayan, R., Garcia, M.R., Lasota, J.P., McClintock, J.E., 1999. Black Hole and Neutron Star Transients in Quiescence. *ApJ* 520, 276–291. doi:10.1086/307443, arXiv:astro-ph/9810323.
- Neopane, S., Bhargava, K., Fisher, R., Ferrari, M., Yoshida, S., Toonen, S., Bravo, E., 2022. Near-Chandrasekhar-mass Type Ia Supernovae from the Double-degenerate Channel. *ApJ* 925, 92. doi:10.3847/1538-4357/ac3b52, arXiv:2111.09890.
- Otoniel, E., Coelho, J.G., Nunes, S.P., Malheiro, M., Weber, F., 2021. Mass limits of the extremely fast-spinning white dwarf CTCV J2056-3014. *A&A* 656, A77. doi:10.1051/0004-6361/202039749, arXiv:2010.12441.
- Pelisoli, I., Brown, A.J., Castro Segura, N., Dhillon, V.S., Dyer, M.J., Garbutt, J.A., Green, M.J., Jarvis, D., Kennedy, M.R., Kerry, P., Littlefair, S.P., McCormac, J., Munday, J., Parsons, S.G., Pike, E., Sahman, D.I., Yates, A., 2025. Constraints on an optical counterpart for the long-period radio transient GPM J1839–10. *MNRAS* 544, L76–L82. doi:10.1093/mnrasl/slaf101, arXiv:2509.20438.
- Pelisoli, I., Marsh, T.R., Buckley, D.A.H., Heywood, I., Potter, S.B., Schwöpe, A., Brink, J., Standke, A., Woudt, P.A., Parsons, S.G., Green, M.J., Kepler, S.O., Munday, J., Romero, A.D., Breedt, E., Brown, A.J., Dhillon, V.S., Dyer, M.J., Kerry, P., Littlefair, S.P., Sahman, D.I., Wild, J.F., 2023. A 5.3-min-period pulsing white dwarf in a binary detected from radio to X-rays. *Nature Astronomy* doi:10.1038/s41550-023-01995-x, arXiv:2306.09272.
- Pelisoli, I., Marsh, T.R., Dhillon, V.S., Breedt, E., Brown, A.J., Dyer, M.J., Green, M.J., Kerry, P., Littlefair, S.P., Parsons, S.G., Sahman, D.I., Wild, J.F., 2022. Found: a rapidly spinning white dwarf in LAMOST J024048.51+195226.9. *MNRAS* 509, L31–L36. doi:10.1093/mnrasl/slab116, arXiv:2108.11396.
- Pétri, J., 2015. Multipolar electromagnetic fields around neutron stars: exact vacuum solutions and related properties. *MNRAS* 450, 714–742. doi:10.1093/mnras/stv598, arXiv:1503.05307.

- Pétri, J., 2019. The illusion of neutron star magnetic field estimates. *MNRAS* 485, 4573–4587. doi:10.1093/mnras/stz711, arXiv:1903.01528.
- Philippov, A., Kramer, M., 2022. Pulsar Magnetospheres and Their Radiation. *ARAA* 60, 495–558. doi:10.1146/annurev-astro-052920-112338.
- Pringle, J.E., Rees, M.J., 1972. Accretion Disc Models for Compact X-Ray Sources. *A&A* 21, 1.
- Raskin, C., Scannapieco, E., Fryer, C., Rockefeller, G., Timmes, F.X., 2012. Remnants of Binary White Dwarf Mergers. *ApJ* 746, 62. doi:10.1088/0004-637X/746/1/62, arXiv:1112.1420.
- Rea, N., Coti Zelati, F., Dehman, C., Hurley-Walker, N., de Martino, D., Bahramian, A., Buckley, D.A.H., Brink, J., Kawka, A., Pons, J.A., Viganò, D., Graber, V., Ronchi, M., Pardo Araujo, C., Borghese, A., Parent, E., Galvin, T.J., 2022. Constraining the Nature of the 18 min Periodic Radio Transient GLEAM-X J162759.5-523504.3 via Multiwavelength Observations and Magneto-thermal Simulations. *ApJ* 940, 72. doi:10.3847/1538-4357/ac97ea, arXiv:2210.01903.
- Rea, N., Hurley-Walker, N., Pardo-Araujo, C., Ronchi, M., Graber, V., Coti Zelati, F., de Martino, D., Bahramian, A., McSweeney, S.J., Galvin, T.J., Hyman, S.D., Dall’Ora, M., 2024. Long-period Radio Pulsars: Population Study in the Neutron Star and White Dwarf Rotating Dipole Scenarios. *ApJ* 961, 214. doi:10.3847/1538-4357/ad165d, arXiv:2307.10351.
- Reding, J.S., Hermes, J.J., Vanderbosch, Z., Dennihy, E., Kaiser, B.C., Mace, C.B., Dunlap, B.H., Clemens, J.C., 2020. An Isolated White Dwarf with 317 s Rotation and Magnetic Emission. *ApJ* 894, 19. doi:10.3847/1538-4357/ab8239, arXiv:2003.10450.
- Rodriguez, A.C., 2025. Spectroscopic detection of a 2.9-hour orbit in a long-period radio transient. *A&A* 695, L8. doi:10.1051/0004-6361/202553684, arXiv:2501.03315.
- Ruderman, M.A., Sutherland, P.G., 1975. Theory of pulsars - Polar caps, sparks, and coherent microwave radiation. *The Astrophysical Journal* 196, 51. doi:10.1086/153393.
- Rueda, J.A., Boshkayev, K., Izzo, L., Ruffini, R., Lorén-Aguilar, P., Külebi, B., Aznar-Siguán, G., García-Berro, E., 2013. A White Dwarf Merger as Progenitor of the Anomalous X-Ray Pulsar 4U 0142+61? *ApJ Lett.* 772, L24. doi:10.1088/2041-8205/772/2/L24, arXiv:1306.5936.
- Rueda, J.A., Ruffini, R., Li, L., Moradi, R., Sahakyan, N., Wang, Y., 2022. The white dwarf binary merger model of GRB 170817A. *International Journal of Modern Physics D* 31, 2230013. doi:10.1142/S0218271822300130, arXiv:2202.00314.
- Rueda, J.A., Ruffini, R., Wang, Y., Bianco, C.L., Blanco-Iglesias, J.M., Karlica, M., Lorén-Aguilar, P., Moradi, R., Sahakyan, N., 2019. Electromagnetic emission of white dwarf binary mergers. *JCAP* 2019, 044. doi:10.1088/1475-7516/2019/03/044, arXiv:1807.07905.
- Ruiter, A.J., Belczynski, K., Fryer, C., 2009. Rates and Delay Times of Type Ia Supernovae. *ApJ* 699, 2026–2036. doi:10.1088/0004-637X/699/2/2026, arXiv:0904.3108.
- Schmidt, G.D., West, S.C., Liebert, J., Green, R.F., Stockman, H.S., 1986. The new magnetic white dwarf PG 1031 + 234 - Polarization and field structure at more than 500 million Gauss. *ApJ* 309, 218–229. doi:10.1086/164593.
- Schreiber, M.R., Belloni, D., Gänsicke, B.T., Parsons, S.G., Zorotovic, M., 2021. The origin and evolution of magnetic white dwarfs in close binary stars. *Nature Astronomy* 5, 648–654. doi:10.1038/s41550-021-01346-8, arXiv:2104.14607.
- Schwab, J., Quataert, E., Kasen, D., 2016. The evolution and fate of super-Chandrasekhar mass white dwarf merger remnants. *MNRAS* 463, 3461–3475. doi:10.1093/mnras/stw2249, arXiv:1606.02300.
- Shen, K.J., 2015. Every Interacting Double White Dwarf Binary May Merge. *ApJ Lett.* 805, L6. doi:10.1088/2041-8205/805/1/L6, arXiv:1502.05052.
- Sousa, M.F., Coelho, J.G., de Araujo, J.C.N., 2020. Gravitational waves from fast-spinning white dwarfs. *Monthly Notices of the Royal Astronomical Society* 492, 5949–5955. doi:10.1093/mnras/staa205, arXiv:2001.08534.
- Sousa, M.F., Coelho, J.G., de Araujo, J.C.N., Guidorzi, C., Rueda, J.A., 2023. On the Optical Transients from Double White-dwarf Mergers. *ApJ* 958, 134. doi:10.3847/1538-4357/ad022f, arXiv:2310.06655.
- Sousa, M.F., Coelho, J.G., de Araujo, J.C.N., Kepler, S.O., Rueda, J.A., 2022. The Double White Dwarf Merger Progenitors of SDSS J2211+1136 and ZTF J1901+1458. *ApJ* 941, 28. doi:10.3847/1538-4357/aca015, arXiv:2208.09506.
- Sousa, M.F., Otoniel, E., Coelho, J.G., de Araujo, J.C.N., 2024. Prospects for the observation of continuous gravitational waves from deformed fast-spinning white dwarfs. *MNRAS* 531, 1496–1505. doi:10.1093/mnras/stae1232, arXiv:2405.02507.
- Stroer, A., Vecchio, A., 2006. The LISA verification binaries. *Classical Quantum Gravity* 23, S809–S817. doi:10.1088/0264-9381/23/19/s19.
- Sturrock, P.A., 1971. A Model of Pulsars. *The Astrophysical Journal* 164, 529. doi:10.1086/150865.
- Tong, H., 2023a. Discussions on the Nature of GLEAM-X J162759.5-523504.3. *ApJ* 943, 3. doi:10.3847/1538-4357/aca7fa, arXiv:2204.01957.

- Tong, H., 2023b. On the nature of long period radio pulsar GPM J1839–10: death line and pulse width. arXiv e-prints, arXiv:2307.14829doi:10.48550/arXiv.2307.14829, arXiv:2307.14829.
- Toonen, S., Hollands, M., Gänsicke, B., Boekholt, T., 2017. The binarity of the local white dwarf population. *Astronomy & Astrophysics* 602, A16.
- Usov, V.V., 1988. Generation of Gamma-Rays by a Rotating Magnetic White Dwarf. *Soviet Astronomy Letters* 14, 258.
- van Kerkwijk, M.H., Chang, P., Justham, S., 2010. Sub-Chandrasekhar White Dwarf Mergers as the Progenitors of Type Ia Supernovae. *ApJ Lett.* 722, L157–L161. doi:10.1088/2041-8205/722/2/L157, arXiv:1006.4391.
- Vennes, S., Schmidt, G.D., Ferrario, L., Christian, D.J., Wickramasinghe, D.T., Kawka, A., 2003. A Multiwavelength Study of the High-Field Magnetic White Dwarf EUVE J0317-85.5 (=RE J0317-853). *ApJ* 593, 1040–1048. doi:10.1086/376728.
- Wang, Z., Rea, N., Bao, T., Kaplan, D.L., Lenc, E., Wadiasingh, Z., Hare, J., Zic, A., Anumalapudi, A., Bera, A., Beniamini, P., Cooper, A.J., Clarke, T.E., Deller, A.T., Dawson, J.R., Glowacki, M., Hurley-Walker, N., McSweeney, S.J., Polisenky, E.J., Peters, W.M., Younes, G., Bannister, K.W., Caleb, M., Dage, K.C., James, C.W., Kasliwal, M.M., Karambelkar, V., Lower, M.E., Mori, K., Ocker, S.K., Pérez-Torres, M., Qiu, H., Rose, K., Shannon, R.M., Taub, R., Wang, F., Wang, Y., Zhao, Z., Bhat, N.D.R., Dobie, D., Driessen, L.N., Murphy, T., Jaini, A., Deng, X., Jahnschindler, J.N., Lee, Y.W.J., Pritchard, J., Tuthill, J., Thyagarajan, N., 2025. Detection of X-ray emission from a bright long-period radio transient. *Nature* 642, 583–586. doi:10.1038/s41586-025-09077-w, arXiv:2411.16606.
- Wickramasinghe, D.T., Ferrario, L., 2000. Magnetism in Isolated and Binary White Dwarfs. *PASP* 112, 873–924. doi:10.1086/316593.
- Xiangyu, Z., Green, G., 2024. Unveiling the milky way dust extinction curve in 3d. URL: <https://doi.org/10.5281/zenodo.11394477>, doi:10.5281/zenodo.11394477. data set.
- Xiao, D., Mészáros, P., Murase, K., Dai, Z.G., 2016. High-energy Neutrino Emission from White Dwarf Mergers. *ApJ* 832, 20. doi:10.3847/0004-637X/832/1/20, arXiv:1608.08150.
- Yoon, S.C., Podsiadlowski, P., Rosswog, S., 2007. Remnant evolution after a carbon-oxygen white dwarf merger. *MNRAS* 380, 933–948. doi:10.1111/j.1365-2966.2007.12161.x, arXiv:0704.0297.
- Zhang, X., Green, G.M., Rix, H.W., 2023. Parameters of 220 million stars from Gaia BP/RP spectra. *MNRAS* 524, 1855–1884. doi:10.1093/mnras/stad1941, arXiv:2303.03420.
- Zhang, X., Jeffery, C.S., 2012. Evolutionary models for double helium white dwarf mergers and the formation of helium-rich hot subdwarfs. *MNRAS* 419, 452–464. doi:10.1111/j.1365-2966.2011.19711.x.
- Zhang, X., Jeffery, C.S., Chen, X., Han, Z., 2014. Post-merger evolution of carbon-oxygen + helium white dwarf binaries and the origin of R Coronae Borealis and extreme helium stars. *MNRAS* 445, 660–673. doi:10.1093/mnras/stu1741, arXiv:1408.5500.
- Zhou, X., Kurban, A., Liu, W.T., Wang, N., Yuan, Y.J., 2025. Nature of Ultralong Period Radio Transients: Could They Be Strange Dwarf Pulsars? *ApJ* 986, 98. doi:10.3847/1538-4357/add268.
- Zhu, C., Chang, P., van Kerkwijk, M.H., Wadsley, J., 2013. A Parameter-space Study of Carbon-Oxygen White Dwarf Mergers. *ApJ* 767, 164. doi:10.1088/0004-637X/767/2/164, arXiv:1210.3616.
- Zhu, H., Tian, W., Li, A., Zhang, M., 2017. The gas-to-extinction ratio and the gas distribution in the Galaxy. *MNRAS* 471, 3494–3528. doi:10.1093/mnras/stx1580, arXiv:1706.07109.